Nonlinear Analysis: Hybrid Systems 61 (2026) 101742

Contents lists available at ScienceDirect

Nonlinear Analysis: Hybrid Systems

journal homepage: www.elsevier.com/locate/nahs

Output-feedback control with wireless channel state detection and actuation message dropout compensation☆,☆☆

Yuriy Zacchia Lun *, Fortunato Santucci, Alessandro D'Innocenzo

Department of Information Engineering, Computer Science and Mathematics, University of L'Aquila, L'Aquila, 67100, Italy

ARTICLE INFO

Keywords:
Control under communication constraints
Resilient networked control systems

ABSTRACT

This paper presents a framework for designing optimal output-feedback controllers that use wireless sensing and actuation links with imperfect channel-state information. Remote system state estimation is performed using a prediction–correction filter that resembles the traditional Kalman filter and incorporates current measurement inputs. The controller computes the current and tentative future control inputs based on the estimated remote system state and the detected wireless channel state. These control inputs are transmitted to actuators as messages. The message dropout compensation strategy for actuation involves scaling the most recent control input when no previously received tentative control inputs are available. We analytically solve finite- and infinite-horizon output-feedback control problems and prove the validity of the separation principle, assuming a reliable mechanism for acknowledging actuation message transmission. We validate the results using an illustrative numerical example that demonstrates the practicality and effectiveness of our framework.

1. Introduction

Wireless networked control systems (WNCSs) are of significant interest to both industry and academia due to their critical applications across various fields, including intelligent transportation, industrial automation, smart grids, and telesurgery, as highlighted in [1,2], and [3].

A considerable focus of WNCS research is on estimation and control over unreliable communication links, as discussed in [1,3,4], and references therein.

This paper extends the work of [5] on state-feedback control with wireless actuation links and imperfect channel state information (CSI) by including wireless sensing links within the output-feedback framework. We address CSI uncertainties using the detector-based method from [6,7], extending it to the one-step-delayed channel-state-observation scenario described by [4,8]. In this setting, finite-state Markov channels (FSMCs, see [9]) model the wireless link dynamics. We use the most general hybrid message dropout compensation (MDC) scheme, which combines transmitting multiple control inputs and scaling inputs to actuators when needed. By integrating the detector-based approach into optimal remote system state estimation, we also substantially expand upon the results of [8]. The *contribution* of this letter is twofold.

☆ This article is part of a Special issue entitled: 'TC 1.5 Networked systems (IFAC WC 2026)' published in Nonlinear Analysis: Hybrid Systems.

☆☆ This work has received funding from the Italian Government under CIPE Resolution No. 70/2017 (Centre of excellence EX-EMERGE) and from the EU under the Horizon Europe programme through grants DigInTraCE (GA 101091801) and Resilient Trust (GA 101112282).

* Corresponding author.

E-mail addresses: yuriy.zacchialun@univaq.it (Y. Zacchia Lun), fortunato.santucci@univaq.it (F. Santucci), alessandro.dinnocenzo@univaq.it (A. D'Innocenzo).

https://doi.org/10.1016/j.nahs.2026.101742
Received 2 November 2025; Received in revised form 1 March 2026; Accepted 14 May 2026

1751-570X/© 2026 The Authors. Published by Elsevier Ltd. This is an open access article under the CC BY license (http://creativecommons.org/licenses/by/4.0/).

1. We address the output-feedback control problem within a comprehensive framework of hybrid actuation MDC and imperfect CSI over unreliable communication links.
2. We design both finite- and infinite-horizon optimal output-feedback controllers, establish the separation principle, and confirm the theoretical findings with a numerical example.

This paper is organized as follows. Section 2 introduces notation and describes the mathematical model of the wireless links that carry data between the controller and the remote system. Section 3 formalizes the complete system model and the control problem. Section 3.5 provides the technical intuition for the solution. Section 4 presents the optimal state estimator. Section 5 summarizes the optimal state-feedback controller. Finally, Section 6 presents the solution to the optimal output-feedback problem as a combination of the results from Sections 4 and 5. Section 7 presents a numerical example to verify the results, and Section 8 summarizes the paper's conclusions.

2. Preliminaries

2.1. Notation

The symbols $\mathbb{R}$, $\mathbb{Z}^+$, and $\mathbb{Z}^{0+}$ represent the sets of real numbers, positive integers, and nonnegative integers, respectively. $\mathbb{R}^n$ denotes n-dimensional Euclidean space. We use $Z \succ 0$ to indicate that Z is a symmetric positive definite matrix, and $Z \succeq 0$ to indicate that it is a symmetric positive semidefinite matrix. The symbol $Z^\top$ represents the transpose of the matrix Z. The spectral radius of a square matrix Z is denoted by $\rho(Z)$. $\mathbb{P}$ represents the probability of an event, and $\mathbb{E}$ denotes the expected value of a random variable. The notation I_N refers to the identity matrix of size N. The symbol $\oplus$ indicates the direct sum, resulting in a diagonal matrix with summands on the main diagonal, while $\otimes$ represents the Kronecker product. Lastly, $\mathbf{0}$ and $\mathbf{1}$ refer to vectors of appropriate sizes, with all elements being zero and one, respectively.

2.2. Wireless link model

In a WNCS, controllers use wireless links to send messages to actuators, while sensors transmit measurements to the controllers. FSMC models effectively capture the time-varying behavior of these wireless links. This section formally describes the FSMC models, including a communication channel state detector, which is necessary for the analyses presented in this article.

Each FSMC consists of a finite set of states $\mathcal{S}_\lambda \triangleq \{s_i^\lambda\}_{i=1}^{N_\lambda}$, where $\lambda \in \{s, a\}$ denotes sensing or actuation link.

Each state can be defined by specific signal-to-interference-plus-noise ratio (SINR) thresholds along with their associated packet dropout probabilities, as noted by [10]. A discrete-time Markov chain determines the active channel state, where the packet dropout probability and transition probabilities depend on the SINR dynamics.

We define sensing and actuation FSMCs formally as follows: $\forall k \in \mathbb{Z}^{0+}$, $\{\theta_k^\lambda\}$ is a (hidden) Markov chain, with

$$\mathbb{P}(\theta_k^\lambda = s_j^\lambda \mid \theta_{k-1}^\lambda = s_i^\lambda) = p_{ij}^\lambda \geq 0, \quad \sum_{j=1}^{N_\lambda} p_{ij}^\lambda = 1. \tag{1}$$

We denote by $\{\delta_k^\lambda\}$ a binary stochastic process that models packet delivery between the transmitter and receiver.

$$\mathbb{P}(\delta_k^\lambda = 1 \mid \theta_k^\lambda = s_j^\lambda) = \hat{\delta}_j^\lambda, \quad \mathbb{P}(\delta_k^\lambda = 0 \mid \theta_k^\lambda = s_j^\lambda) = 1 - \hat{\delta}_j^\lambda, \tag{2}$$

and the column vector $\hat{\delta}^\lambda \triangleq [\hat{\delta}_j^\lambda]_{j=1}^{N_\lambda}$ contains the probabilities of successful packet transmission, which depend on the channel state. We group channel state transition probabilities in the transition probability matrix P_c^λ, and we present the success (or, conversely, failure) probabilities of delivering a packet at time k in the following matrices.

$$P_s^\lambda \triangleq [p_{ij}^\lambda \hat{\delta}_j^\lambda]_{i,j=1}^{N_\lambda}, \quad P_f^\lambda = P_c^\lambda - P_s^\lambda, \quad P_c^\lambda \triangleq [p_{ij}^\lambda]_{i,j=1}^{N_\lambda}. \tag{3}$$

We also denote the channel state probability at time k as

$$\mathbb{P}(\theta_k^\lambda = s_i^\lambda) = \pi_i^\lambda(k). \tag{4}$$

Wireless receivers perform CSI measurements, which can be sent back to the transmitters. In sensing links, the controller acts as the receiver and directly accesses the measured CSI. Conversely, in actuation links, the controller is the transmitter. The transmitter usually acquires the measured CSI through a reporting mechanism that resembles an acknowledgment of transmission outcomes, introducing a delay.

Similar to [5], we employ a detector-based approach to investigate the impact of CSI measurement noise, including specific cases where FSMC states are partially or not observed at all. Specifically, $\hat{\theta}_k^\lambda \in \{\hat{s}_\mu^\lambda\}_{\mu=1}^{M_\lambda}$ represents the measured CSI from a detector, using an emission probability matrix (EPM), P_e^λ, defined as follows.

$$\mathbb{P}(\hat{\theta}_k^\lambda = \hat{s}_\mu^\lambda \mid \theta_k^\lambda = s_i^\lambda) = \alpha_{i\mu}^\lambda \geq 0, \ \sum_{\mu=1}^{M_\lambda} \alpha_{i\mu}^\lambda = 1, \quad P_e^\lambda \triangleq \left[\alpha_{i\mu}^\lambda\right]_{i,\mu=1}^{N_\lambda, M_\lambda}. \tag{5}$$

$M_\lambda \leq N_\lambda$ includes the following particular cases:

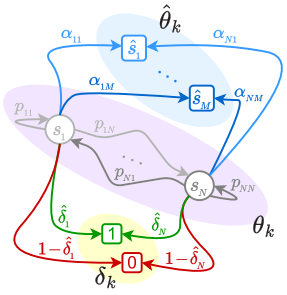

Fig. 1. Wireless communication link model.

- *Perfect CSI*: $M_\lambda = N_\lambda$, $P_e^\lambda = I_{N_\lambda}$ so that θ_k^λ is known.
- *No CSI*: $M_\lambda = 1$, $P_e^\lambda = \mathbf{1}$ so that θ_k^λ is unknown.

Additionally, the scenario of partial observation with clusters is effectively illustrated by a detector where $M_\lambda < N_\lambda$, as discussed in [6] and in Section 7.

For notational convenience, we denote the CSI detector's state space for a link λ as $\hat{S}_\lambda \triangleq \{\hat{s}_\mu^\lambda\}_{\mu=1}^{M_\lambda}$.

As a practical example of a communication channel state detector, we consider the maximum-likelihood estimator, which outputs the state with the highest emission probability. Formally, let e_i^λ denote the column vector of the standard basis of $\mathbb{R}^{N_\lambda}$ (all its components are zero except the ith, which equals one). Then,

$$\hat{\theta}_k^\lambda = \max\left(\left(e_{\theta_k^\lambda}^\lambda\right)^\top P_e^\lambda\right). \tag{6}$$

Fig. 1 summarizes our FSMC model for a wireless communication link. The shaded regions highlight the state spaces of the key variables: the hidden Markov state θ_k, the detected link state $\hat{\theta}_k$, and the transmission outcome δ_k. We omitted the superscripts and subscripts λ to simplify the description, noting that all elements in the figure refer to the same link. The gray circles, s_1 and s_N, within the violet region represent the hidden states of the Markov chain, and the gray arrows indicate the transition probabilities between these states, as defined in (1). The green and red rounded squares, labeled 1 and 0, within the yellow region represent the outcomes of the message transmission. These outcomes depend on the hidden Markov states, as indicated by the green and red arrows emanating from those states, with probabilities given by (2). The hidden Markov states are observed by the link state detector, and the detected states, $\hat{s}_1$ and $\hat{s}_M$, are shown as blue rounded squares within the light-blue region. The blue arrows emanating from hidden Markov states indicate the emission probabilities defined in (5).

For ease of notation, we define the diagonal matrices

$$P_\pi^\lambda(k) = \bigoplus_{i=1}^{N} \pi_i^\lambda(k), \quad P_\alpha^\lambda(\mu) = \bigoplus_{i=1}^{N} \alpha_{i\mu}^\lambda. \tag{7}$$

These matrices will allow us to concisely describe the transition probabilities among the operational modes of the closed-loop system, as detailed in Sections 4 and 5.

3. System model

This section presents the complete system model and the control problem.

3.1. Closed-loop system components

We are examining a discrete-time linear stochastic system

$$x_{k+1} = Ax_k + Bu_k + w_k. \tag{8}$$

The system state $x_k \in \mathbb{R}^{n_x}$ and the control input $u_k \in \mathbb{R}^{n_u}$. A and B represent the respective state and input matrices. The process noise w_k is a white Gaussian noise with zero mean and covariance matrix Σ_w. The initial conditions are

$$\mathbb{E}\left(x_0\right) = \mathrm{x}_0, \ \mathbb{E}\left(x_0 x_0^\top\right) = \mathrm{X}_0. \tag{9}$$

The measured output $y_k \in \mathbb{R}^{n_y}$ is defined as

$$y_k = Cx_k + v_k, \tag{10}$$

where C is the output matrix of appropriate size, and v_k is a white Gaussian measurement noise having zero mean and covariance matrix Σ_v. This output is transmitted to the controller over the sensing link. This link is part of the wireless communication layer

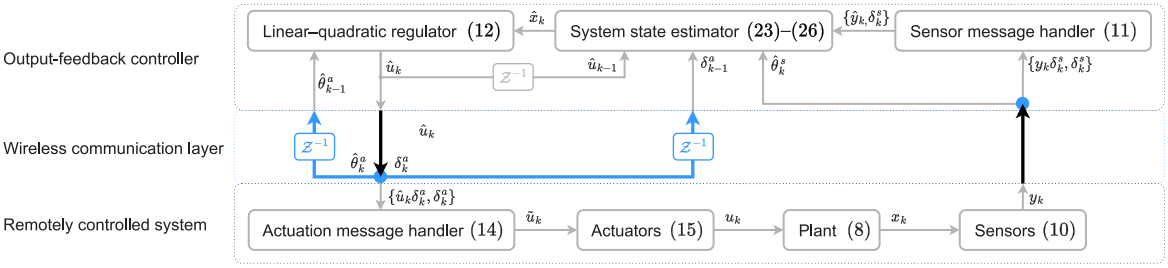

Fig. 2. The closed-loop system architecture.

that connects the output-feedback controller to the remote system via sensing and actuation data links, whose formal models are presented in Section 2.2. The controller comprises the sensor message handler described below, the remote system state estimator (SE) described in Section 4, and the linear–quadratic regulator presented in Section 5. These three components are collocated, which prevents data loss between them.

The sensor message handler verifies the outcome of sensor message transmission, represented by the binary stochastic variable δ_k^s. It then computes the updated sensor data input to SE using the zero-input MDC:

$$\hat{y}_k = \delta_k^s y_k. \tag{11}$$

If the sensor message is received correctly, $\delta_k^s = 1$ and $\hat{y}_k = y_k$. Otherwise, if the sensor message is corrupted or lost, $\delta_k^s = 0$, and $\hat{y}_k = \mathbf{0}$.

Both δ_k^s and $\hat{y}_k$ are used by the SE to compute the current state estimate $\hat{x}_k$ and the one-step prediction of the next state estimate $\bar{x}_{k+1}$. After receiving δ_{k+1}^s and $\hat{y}_{k+1}$, the SE corrects the predicted state estimate $\bar{x}_{k+1}$ in the next iteration, producing the updated state estimate $\hat{x}_{k+1}$. Notably, the updated state estimate matches the predicted estimate when no update is available due to sensor message loss or corruption: if $\delta_{k+1}^s = 0$, then $\hat{y}_{k+1} = \mathbf{0}$ and $\hat{x}_{k+1} = \bar{x}_{k+1}$.

The output of the SE at discrete time k is the estimated state $\hat{x}_k$, which the linear–quadratic regulator (LQR) uses to compute an actuation message $\hat{u}_k$ comprising the current control input $\bar{u}_{(k|k)}$ and $n_f \in \mathbb{Z}^{0+}$ future inputs to account for possible actuation message dropouts after the current transmission.

$$\hat{u}_k^\top = [\bar{u}_{(k+f|k)}^\top]_{f=0}^{n_f},\ \bar{u}_{(k+f|k)} = K_{(k+f,\hat{\theta}_{k-1}^a)}\hat{x}_k. \tag{12}$$

The actuation message is transmitted to the controlled system via the actuation link. As indicated in Section 2.2, the controller is the transmitter, so it may acquire the actuation link state detected during the previous transmission ($\hat{\theta}_{k-1}^a$) and use it to compute or select the appropriate control gains in (12). Notably, if the actuation link state is unknown, $P_e^a = \mathbf{1}$ in (5), and (12) remains valid.

The actuation message handler is located at the receiving end of the link. It verifies the outcome of actuation message transmission, represented by the binary stochastic variable δ_k^a, and then applies the hybrid MDC strategy [5], which corresponds to generalized MDC at the last available control input when the actuation message dropout interval exceeds the number of anticipated tentative control inputs, n_f. In particular, this input is multiplied by the matrix $\boldsymbol{\Phi} = \bigoplus_{i=1}^{n_u} \phi_i$, with $0 \le \phi_i \le 1$. This matrix is also known as the generalized MDC factor [4]. The actuation message handler using the hybrid MDC maintains a buffer $\tilde{u}_k$, formally defined as follows. Let $\tilde{e}_i$ indicate the column vector of the standard basis of $\mathbb{R}^{n_f+1}$.

$$H \triangleq \sum_{i=1}^{n_f} \tilde{e}_i \otimes \tilde{e}_{i+1}^\top \otimes I_{n_u} + \tilde{e}_{n_f+1} \otimes \tilde{e}_{n_f+1}^\top \otimes \boldsymbol{\Phi}. \tag{13}$$

$$\tilde{u}_k = \delta_k^a \hat{u}_k + \left(1 - \delta_k^a\right) H \tilde{u}_{k-1},\ \tilde{u}_{-1} = \mathbf{0}. \tag{14}$$

If an actuation message is successfully received, then $\delta_k^a = 1$, and the buffer stores the actuation message. Otherwise, the buffer undergoes a linear transformation of its content using the matrix H. This transformation removes the first n_u elements, shifts all the remaining elements by n_u positions upwards, multiplies the last n_u elements by $\boldsymbol{\Phi}$, and stores the result at the bottom of the buffer.

Finally, the control inputs consist of the first n_u elements of the buffer $\tilde{u}_k$:

$$u_k = F\tilde{u}_k,\ F \triangleq \tilde{e}_1^\top \otimes I_{n_u}. \tag{15}$$

Fig. 2 summarizes the closed-loop system architecture. The system comprises the remotely controlled system and its output-feedback controller at the application layer, connected through a wireless communication layer. Gray rounded rectangles represent the main components and reference the equations that define them. Thin gray arrows indicate interconnections among the components and specify their inputs and outputs. Thick black arrows indicate message transmission over wireless data links, whereas thick blue arrows indicate CSI and acknowledgment feedback.

Fig. 3 shows the timing of the application data flow between the remote system and its output-feedback controller. Thick black arrows indicate message transfer via wireless data links, while thin gray arrows represent local data movement within the application. The data from the communication layer is omitted to keep the diagram clear.

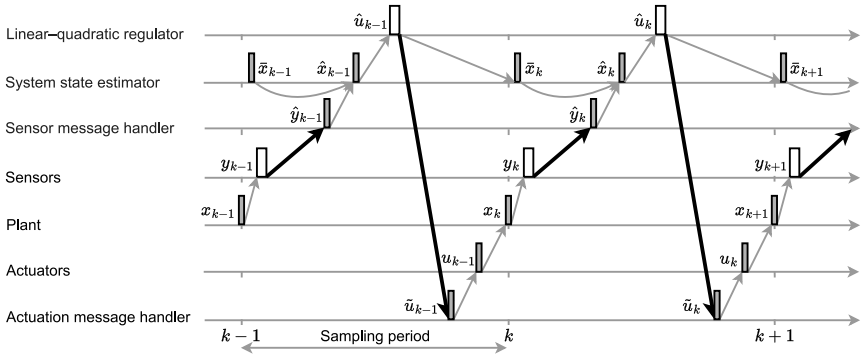

Fig. 3. The control application data flow.

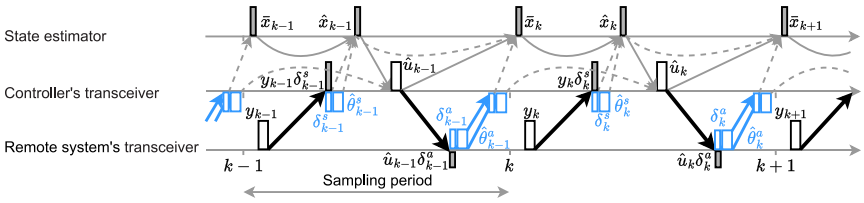

Fig. 4. The communication layer data flow.

Remark 1. The system dynamics in (8) follow the standard state-space form and implicitly include input delays caused by communication and processing, as shown in Fig. 3. Refer to [11] and their references for technical details on incorporating input delays into the standard state-space form.

Fig. 4 illustrates the timing of data transfer between the remote system and the output-feedback controller, specific to the wireless communication layer. Thick blue arrows indicate CSI and transmission acknowledgment feedback, such as the automatic repeat request (ARQ) mechanism. Thin dashed arrows show the subsequent data flow within the control application.

The CSI measurements are performed at the communication layer. This layer also provides a reliable acknowledgment of transmission outcomes, allowing us to make the following common technical assumption.

Assumption 1. The SE knows δ^a_{k-1} at each k, i.e., whether the actuators have received the previously sent messages.

Remark 2. Both Assumption 1 and access to the measured CSI require the output-feedback controller to interact with the communication layer, leading to cross-layer optimization and even coupled design.

Remark 3. Implementing an actuation message acknowledgment mechanism at the control application layer would require an additional data link similar to the sensing data link. As a data link, it may be unreliable, so Assumption 1 will not hold. Furthermore, the sensing and acknowledgment data links would involve the same transmitters and receivers using the same communication resources — such as frequency bands and transmit power — in the same communication environment, and thus could be correlated.

3.2. Information set

The information set available to the output-feedback controller for the computation of the remote system state estimate and the current and tentative future control inputs in (12) is as follows.

$$\mathcal{I}^{lqr}_k = \left\{ \left(\hat{x}_t\right)_{t=0}^{k}, \left(\hat{\theta}^a_{t-1}\right)_{t=1}^{k} \right\}, \tag{16a}$$

$$\hat{\mathcal{I}}^{se}_k = \left\{ \left(\bar{x}_t\right)_{t=0}^{k}, \left(\hat{y}_t\right)_{t=0}^{k}, \left(\delta^s_t\right)_{t=0}^{k}, \left(\hat{\theta}^s_t\right)_{t=0}^{k} \right\}, \tag{16b}$$

$$\bar{\mathcal{I}}^{se}_k = \left\{ \left(\hat{y}_{t-1}\right)_{t=1}^{k}, \left(\delta^s_{t-1}\right)_{t=1}^{k}, \left(\hat{\theta}^s_{t-1}\right)_{t=1}^{k}, \left(\delta^a_{t-1}\right)_{t=1}^{k}, \left(\hat{u}_{t-1}\right)_{t=1}^{k} \right\}, \tag{16c}$$

$$\mathcal{I}_k = \mathcal{I}^{lqr}_k \cup \hat{\mathcal{I}}^{se}_k \cup \bar{\mathcal{I}}^{se}_k. \tag{16d}$$

where $\mathcal{I}^{lqr}_k$, $\hat{\mathcal{I}}^{se}_k$, $\bar{\mathcal{I}}^{se}_k$, and $\mathcal{I}_k$ represent the information sets of the LQR, SE for the correction and prediction steps, and the overall output-feedback controller, respectively. The contents of the respective sets are shown in Fig. 4 for $t = k$: $\mathcal{I}^{lqr}_k$ contains the variables

on the left-hand side of $\hat{u}_k$ that are connected to $\hat{u}_k$ with gray arrows; $\hat{\mathcal{I}}_k^{se}$ includes the variables on the left-hand side of $\hat{x}_k$ that are directly connected to it; and $\bar{\mathcal{I}}_k^{se}$ comprises the variables on the left-hand side of $\bar{x}_k$ that are connected to $\bar{x}_k$ with gray solid or dashed arrows. $\bar{x}_k$ and $\hat{x}_k$ are internal variables involved in the intermediate steps of calculating the actuation message $\hat{u}_k$, as indicated by the solid gray arrows in Fig. 4. $\bar{\mathcal{I}}_k^{se}$ is used to compute $\bar{x}_k$, which is part of $\hat{\mathcal{I}}_k^{se}$ and is used to compute $\hat{x}_k$. $\hat{x}_k$ is then used to compute $\hat{u}_k$. Consequently, we explicitly specify the information set used by the output-feedback controller to compute $\hat{u}_k$ as a combination of external variables employed throughout all intermediate steps:

$$\mathcal{I}_k = \left\{ \left(\hat{y}_t\right)_{t=0}^{k}, \left(\delta_t^s\right)_{t=0}^{k}, \left(\hat{\theta}_t^s\right)_{t=0}^{k} \left(\delta_{t-1}^a\right)_{t=1}^{k}, \left(\hat{\theta}_{t-1}^a\right)_{t=1}^{k}, \left(\hat{u}_{t-1}\right)_{t=1}^{k} \right\}. \tag{17}$$

Remark 4. The information used for linear–quadratic regulation includes the CSI detected by the actuator's receiver, rather than the actual state of the wireless channel. Additionally, as a transmitter, the controller does not measure CSI on the actuation link and cannot determine the outcome of a control message transmission before sending it. Therefore, this information is accessible with a one-step delay. As a receiver, the SE is aware of the outcome of the sensor message transmission and the CSI measured on the sensing link. However, the measured CSI depends on the detector's EPM and may be imperfect or unavailable.

Remark 5. While information sets in (16) include the entire history of the relevant variables, the LQR and the SE use only the most recent values.

3.3. Technical assumptions

In addition to the variables in (17), the output-feedback controller knows the system's parameters, as formalized by the following standard technical assumption.

Assumption 2. Both the LQR and the SE know the matrices A, B, C, H, and F.

As in [5,8,12], and references therein, we also make the following technical assumptions.

Assumption 3. The discrete-time Markov chains $\{\theta_k^s\}$ and $\{\theta_k^a\}$, and the noise processes $\{w_k\}$ and $\{v_k\}$, are independent of each other and of the initial condition x_0. Furthermore, the noise processes $\{w_k\}$ and $\{v_k\}$ and the initial condition x_0 are independent of the binary stochastic processes $\{\delta_k^s\}$ and $\{\delta_k^a\}$ and of the CSI detectors' outputs $\{\hat{\theta}_k^s\}$ and $\{\hat{\theta}_k^a\}$.

Assumption 4. The covariance matrix of the measurement noise is positive definite, i.e., $\Sigma_v \succ 0$.

The infinite-horizon case also requires an additional ergodicity assumption, as formally stated below.

Assumption 5. Markov chains $\{\theta_k^a\}$ and $\{\theta_k^s\}$ are ergodic. Their steady-state probability distributions are

$$\pi_{(\infty)}^{\lambda} = [\pi_i^{\lambda}(\infty)]_{i=1}^{N_\lambda}, \ \pi_i^{\lambda}(\infty) = \lim_{k\to\infty} \pi_i^{\lambda}(k), \ \lambda \in \{s, a\}. \tag{18}$$

3.4. Problem statement

Let $T \in \mathbb{Z}^+ \cup \{\infty\}$ represent a control time horizon and $\vec{u}_T^{\,n_f}$ be a sequence of length T of control messages as in (12),

$$\vec{u}_T^{\,n_f} = \left(\hat{u}_t\right)_{t=0}^{T-1}. \tag{19}$$

Let $\mathcal{U}_T^{n_f}$ denote the set of all possible sequences defined by (19). For any given pair of state-weighting and input-weighting matrices $Q \succeq 0$ and $R \succ 0$ of appropriate size, we consider the following cost functions. For $T < \infty$,

$$J_T\left(\mathcal{U}_T^{n_f}, \mathrm{x}_0, \mathrm{X}_0\right) = \mathbb{E}\left(x_T^\top Q x_T + \sum_{k=0}^{T-1} \left(x_k^\top Q x_k + u_k^\top R u_k \right) \mid \mathcal{I}_0 \right). \tag{20}$$

Remark 6. The cost (20) weights the control inputs, which depend on $\vec{u}_T^{\,n_f}$, $\{\delta_k^a\}$, and Φ through (13)–(15).

The infinite-horizon cost is defined for $T = \infty$ as follows.

$$J_\infty\left(\mathcal{U}_T^{n_f}, \mathrm{x}_0, \mathrm{X}_0\right) = \limsup_{T\to\infty} \frac{1}{T} J_T\left(\mathcal{U}_T^{n_f}, \mathrm{x}_0, \mathrm{X}_0\right). \tag{21}$$

This paper addresses the following design problems.

Problem 1 (*Finite-Horizon Case*)**.** Given a system (8)–(15) with communication links described by (1)–(6), design a controller that minimizes the cost (20) under Assumptions 1–4 and the information set (17).

Problem 2 (*Infinite-Horizon Case*)**.** For a system (8)–(15) with communication links described by (1)–(6), design a controller that minimizes the cost (21) under Assumptions 1–5 and the information set (17).

3.5. Technical insights for the problem solution

In the remainder of this paper, we solve Problems 1 and 2 within the general Markov jump linear system (MJLS) framework and its underlying principles.

Output-feedback control for MJLSs has been investigated in [13,14], where the same Markov chain drives the dynamics of the controlled system (also referred to as a process or plant), the system state estimator, and the state-feedback controller, with no delay or observation imperfections in the operational mode.

By drawing a comparison with the classical linear–quadratic–Gaussian (LQG) control problem, [13] presents a result that mirrors the separation principle for optimal control of linear systems. The separation principle, formally known as the principle of separation of estimation and control, states that the solution to the optimal control problem for linear systems with output measurements and a quadratic cost is similar to the linear–quadratic regulation case, except that the state variable is replaced by its estimate from the Kalman filter. Therefore, the LQG problem can be decomposed into two distinct parts. [13] shows that the separation principle also holds in the MJLS setting, where the optimal Markov jump output-feedback controller can be designed from two sets of coupled difference (for the finite-horizon case) and algebraic (for the infinite-horizon case) Riccati equations, one associated with the control problem and the other with the filtering problem.

The optimal Markov-jump filtering problem in [13] was recently revisited in [12], which incorporated a correction step that accounts for the most recent system-state measurement. Specifically, [12] shows that the proposed prediction–correction filter is the optimal Markovian filter when the system operational mode is perfectly observed. When there is only one mode of operation, the results in [12] coincide with those of the traditional Kalman filter for discrete-time linear systems.

At the same time, [8] obtained similar results for WNCSs with two independent, perfectly observed FSMCs and a zero-input MDC. In particular, [8] presents a prediction–correction filter, the current estimator, as the optimal solution to the filtering problem and proves that the separation principle remains valid when reliable acknowledgment messages convey the one-step-delayed CSI of the actuation link and the outcome of the corresponding transmission.

Subsequent works on optimal state-feedback control of WNCSs [4,15], and [5] focused on the actuation MDC, addressing generalized and hybrid MDC in various settings. [4] derived finite- and infinite-horizon LQR solutions under one-step-delayed perfect CSI, generalized MDC, and known FSMC state-transition probabilities. [15] extended the finite-horizon LQR results in [4] to a polytopic, time-inhomogeneous setting, where FSMC state-transition probabilities are time-varying and unknown, yet bounded within a convex set of vertices. Finally, [5] extended the results in [4] to hybrid MDC and one-step-delayed imperfect CSI.

This paper generalizes the results in [5,8] within a unified framework for optimal output-feedback control under imperfect CSI and a hybrid actuation MDC, demonstrating that the separation principle between estimation and control remains valid, provided that the SE knows whether the controlled system has received prior actuation messages. This generalization presents several technical challenges: imperfect CSI requires careful characterization of the filter's operational modes, especially the transition probabilities among them, and the lasting effect of the hybrid actuation MDC on the control inputs must be incorporated into the filter's design. Then, the Markovian nature of wireless links, as described in Section 2.2, enables us to develop a practical hidden MJLS model of the closed-loop system and to specialize the MJLS theory from [12,13] to this general WNCS setting.

Any infinite-horizon output-feedback control strategy aims to ensure that the closed-loop system's state converges to an equilibrium point, which is zero in the noiseless setting (i.e., in (8) and (10), $w_k = 0$ and $v_k = 0$ $\forall k \in \mathbb{Z}^{0+}$). For MJLSs, this goal corresponds to mean-square (MS) stability, which is equivalent to both exponential MS stability and stochastic stability [4, Remark 11]. Consequently, we recall only the definition of MS stability:

Definition 1 (*Mean-Square Stability*)**.** The system (8)–(15), under (1)–(6), is MS stable if there exist equilibrium points x_e and X_e, independent of the initial condition $(x_0, \theta_0^s, \theta_0^a)$, such that the following holds $\forall(x_0, \theta_0^s, \theta_0^a)$:

$$\lim_{k\to\infty} \|\mathbb{E}(x_k) - x_e\| = 0, \quad \lim_{k\to\infty} \|\mathbb{E}(x_k x_k^\top) - X_e\| = 0. \tag{22}$$

In (22), $\|\cdot\|$ indicates an arbitrary matrix norm. In the following, $\|\cdot\|^2$ will refer to the Euclidean norm.

MS stability in Definition 1 implicitly requires the existence of an appropriate infinite-horizon SE (the property known as MS detectability, formally defined in Section 4.4) and an infinite-horizon LQR (the property known as MS stabilizability, formally defined in Section 5.2).

We solve Problems 1 and 2 in three steps: we first assume the separation principle holds and separately design the optimal SE in Section 4 and the optimal LQR in Section 5; then, in Section 6, we combine them and prove that the separation principle holds. This approach is driven by the problem's complexity, necessitating a thorough analysis of estimation and control to fully understand the complete solution.

4. Prediction–correction filter

This section presents the optimal SE for the system (8)–(15) under (1)–(6), (16b), and (16c), and for arbitrary sequences of control messages defined by (12) and (19). It is an integral part of the output-feedback control solution described in Section 6. Section 4.1 describes the SE structure, Section 4.2 analyzes the SE error dynamics, and Sections 4.3 and 4.4 present optimal SE prediction and correction gains for finite- and infinite-horizon settings.

4.1. State estimator structure

This section describes the state estimation procedure and emphasizes the structural adjustments required to ensure the validity of the separation principle. The prediction and correction steps described below align with those in [12], enabling the adaptation of their results to the WNCS setting in this paper, as detailed in Appendix F.

Like the traditional Kalman filter, this SE aims to minimize the mean-square error of the estimate, represented by $\sum_{k=0}^{T} \mathbb{E}\left(\|x_k - \hat{x}_k\|^2\right)$ for the finite-horizon case and by $\liminf_{k\to\infty} \mathbb{E}\left(\|x_k - \hat{x}_k\|^2\right)$ for the infinite-horizon case. This SE repeats a two-step process: the first step predicts the filter's next state from the current state and available measurements, and the second step updates the state estimate by correcting the predicted state with the current measurements.

As in the classical LQG setting, the key requirement for the validity of the separation principle is the filter's knowledge of the control inputs applied to the plant: when the SE knows these inputs, it can compensate for them, so that they do not contribute to the estimation error. However, control inputs $\left(u_t\right)_{t=0}^{k}$ defined by (15) are not a part of the filter's information set defined by (16b), and (16c). Therefore, the optimal SE for a system (8)–(15) constrained by (1)–(6), (16b), and (16c) requires an additional phase that reconstructs a local copy of the actuation MDC buffer (14) to prevent estimation errors from control inputs. This local copy is described as follows.

$$\breve{u}_k = \delta_k^a \hat{u}_k + \left(1 - \delta_k^a\right) H \breve{u}_{k-1},\ \breve{u}_{-1} = \mathbf{0}. \tag{23}$$

It allows the SE to infer the previous control inputs applied to the plant, as formalized below.

Proposition 1. *Under Assumption 2, an SE with information set (16c) can unequivocally determine the control inputs* $\left(u_{t-1}\right)_{t=1}^{k}$ *via (23) as* $\left(F\breve{u}_{t-1}\right)_{t=1}^{k}$.

Proof. See Appendix A. □

The SE's state $\bar{x}_k$ is the one-step prediction of the current state estimate from the previous step, subject to (16c):

$$\bar{x}_k = A\bar{x}_{k-1} + BF\breve{u}_{k-1} - G_{(k-1,\hat{\theta}^s_{k-1})}\left(\hat{y}_{k-1} - \delta^s_{k-1} C\bar{x}_{k-1}\right) \tag{24}$$

describes the *prediction step*, in which the second addend compensates for the effect of the control inputs as per Proposition 1. $G_{(k-1,\hat{\theta}^s_{k-1})}$ is the sensing link-state-dependent filter gain (to be found). We call it the prediction gain.

The *initial state* of the SE is the system's expected initial state, as in (9):

$$\bar{x}_0 = \mathrm{x}_0. \tag{25}$$

The *correction step* provides the remote system's current state estimate using the information in (16b):

$$\hat{x}_k = \bar{x}_k - \hat{G}_{(k,\hat{\theta}^s_k)}\left(\hat{y}_k - \delta^s_k C\bar{x}_k\right), \tag{26}$$

where $\hat{G}_{(k,\hat{\theta}^s_k)}$ is another sensing link-state-dependent filter gain (to be determined), which we call the correction gain.

To derive the analytical expressions for the prediction and correction gain matrices $G_{(k,\hat{\theta}^s_k)}$ and $\hat{G}_{(k,\hat{\theta}^s_k)}$ in the optimal SE, we will first show that the prediction and estimation errors of the SE described by (23)–(26) evolve as an MJLS independent of the control input. Then, we will adapt the relevant results from the general MJLS theory in [12] to the problem at hand.

4.2. State estimate error dynamics

This section describes the error dynamics of the system state estimate and shows that these dynamics evolve as an MJLS. Throughout the remainder of this paper, we denote the SE's prediction error at discrete time k as $\tilde{x}_k$:

$$\tilde{x}_k \triangleq x_k - \bar{x}_k. \tag{27}$$

From (8), (10), (11), (15), (24), and Proposition 1, we obtain the following expression for the SE's prediction error dynamics:

$$\tilde{x}_k = \left(A + \delta^s_{k-1} G_{(k-1,\hat{\theta}^s_{k-1})} C\right)\tilde{x}_{k-1} + \delta^s_{k-1} G_{(k-1,\hat{\theta}^s_{k-1})} v_{k-1} + w_{k-1}. \tag{28}$$

From (26), (10), (11), (28), the error in the current state estimate at discrete time k is given by

$$x_k - \hat{x}_k = \left(I_{n_x} + \delta^s_k \hat{G}_{(k,\hat{\theta}^s_k)} C\right)\tilde{x}_k + \delta^s_k \hat{G}_{(k,\hat{\theta}^s_k)} v_k. \tag{29}$$

The error dynamics in (28) and (29) depend on the sensing FSMC, as described by (1)–(6), with $\lambda = s$. Thus, we combine the outcome of the last sensor message transmission and the most recent detected CSI for the sensing link into an augmented discrete state:

$$\eta^s_k \triangleq (\delta^s_k, \hat{\theta}^s_k). \tag{30}$$

Stochastic process $\left\{\eta^s_k\right\}$ is a Markov chain with the following transition probabilities.

Let $\hat{e}^\lambda_i$ indicate the column vector of the standard basis of $\mathbb{R}^{M_\lambda}$, with $\lambda \in \{s, a\}$.

Proposition 2. *Transition probabilities between the states defined by (30) are*

$$\mathbb{P}\left(\eta^s_{k+1} = (1, \hat{s}^s_\nu) \mid \eta^s_k = (\beta, \hat{s}^s_\mu)\right) = \frac{\hat{e}^{s\top}_\mu P^{s\top}_e P^s_\pi(k) P^s_s P^s_e \hat{e}^s_\nu}{\hat{e}^{s\top}_\mu P^{s\top}_e P^s_\pi(k)\mathbf{1}}, \quad \mathbb{P}\left(\eta^s_{k+1} = (0, \hat{s}^s_\nu) \mid \eta^s_k = (\beta, \hat{s}^s_\mu)\right) = \frac{\hat{e}^{s\top}_\mu P^{s\top}_e P^s_\pi(k) P^s_f P^s_e \hat{e}^s_\nu}{\hat{e}^{s\top}_\mu P^{s\top}_e P^s_\pi(k)\mathbf{1}}. \tag{31}$$

Proof. See Appendix B.

Remark 7. The transition probabilities in (31) are independent of β, which is the binary value of δ^s_k.

For notational convenience, we denote the expressions of the transition probabilities in (31) as follows.

$$\zeta^s_{(k,\mu,1,\nu)} \triangleq \frac{\hat{e}^{s\top}_\mu P^{s\top}_e P^s_\pi(k) P^s_s P^s_e \hat{e}^s_\nu}{\hat{e}^{s\top}_\mu P^{s\top}_e P^s_\pi(k)\mathbf{1}}, \quad \zeta^s_{(k,\mu,0,\nu)} \triangleq \frac{\hat{e}^{s\top}_\mu P^{s\top}_e P^s_\pi(k) P^s_f P^s_e \hat{e}^s_\nu}{\hat{e}^{s\top}_\mu P^{s\top}_e P^s_\pi(k)\mathbf{1}}. \tag{32}$$

Corollary 1. *In the perfect CSI case, (31) becomes*

$$\mathbb{P}\left(\eta^s_{k+1} = \left(1, \hat{s}^s_\nu = s^s_j\right) \mid \eta^s_k = \left(\beta, \hat{s}^s_\mu = s^s_i\right)\right) = p^s_{ij}\hat{\delta}^s_j, \quad \mathbb{P}\left(\eta^s_{k+1} = \left(0, \hat{s}^s_\nu = s^s_j\right) \mid \eta^s_k = \left(\beta, \hat{s}^s_\mu = s^s_i\right)\right) = p^s_{ij}\left(1 - \hat{\delta}^s_j\right).$$

Proof. See Appendix C.

Corollary 2. *In the no CSI case, (31) is transformed into*

$$\mathbb{P}\left(\eta^s_{k+1} = (1, -) \mid \eta^s_k = (\beta, -)\right) = \mathbf{1}^\top P^s_\pi(k) P^s_s \mathbf{1}, \quad \mathbb{P}\left(\eta^s_{k+1} = (0, -) \mid \eta^s_k = (\beta, -)\right) = \mathbf{1}^\top P^s_\pi(k) P^s_f \mathbf{1},$$

where "−" indicates that the CSI is unavailable.

Proof. See Appendix D.

Corollary 3. *Under Assumption 5, for $\gamma \in \{0, 1\}$,*

$$\lim_{k\to\infty} \zeta^s_{(k,\mu,\gamma,\nu)} = \zeta^s_{(\infty,\mu,\gamma,\nu)}, \tag{33}$$

whose expression is (32) having ∞ instead of k.

Proof. It is a direct consequence of Assumption 5.

A complete description of the Markov chain $\{\eta^s_k\}$ requires deriving the state probabilities, as detailed below.

Proposition 3. *Probabilities of the states in (30) are*

$$\mathbb{P}\left(\eta^s_k = \left(1, \hat{s}^s_\mu\right)\right) = \hat{\delta}^{s\top} P^s_\pi(k) P^s_e \hat{e}^s_\mu, \quad \mathbb{P}\left(\eta^s_k = \left(0, \hat{s}^s_\mu\right)\right) = \left(\mathbf{1} - \hat{\delta}^s\right)^\top P^s_\pi(k) P^s_e \hat{e}^s_\mu, \tag{34}$$

Proof. See Appendix E.

Corollary 4. *In the perfect CSI case, (34) becomes*

$$\mathbb{P}\left(\eta^s_k = \left(1, \hat{s}^s_\nu = s^s_j\right)\right) = \hat{\delta}^s_j \pi_j(k), \quad \mathbb{P}\left(\eta^s_k = \left(0, \hat{s}^s_\nu = s^s_j\right)\right) = \left(1 - \hat{\delta}^s_j\right)\pi_j(k).$$

Proof. It is a direct result of $P^s_e = I_{N_s}$. □

Corollary 5. *In the no CSI case, (34) is transformed into*

$$\mathbb{P}\left(\eta^s_k = (1, -)\right) = \hat{\delta}^{s\top} P^s_\pi(k)\mathbf{1}, \quad \mathbb{P}\left(\eta^s_k = (0, -)\right) = \left(\mathbf{1} - \hat{\delta}^s\right)^\top P^s_\pi(k)\mathbf{1}.$$

where "−" indicates that the CSI is unavailable.

Proof. It is a direct result of $P^s_e = \mathbf{1}$ and $\hat{e}^s_\nu = 1$. □

For notational convenience, we denote the expressions of the state probabilities in (34) as follows.

$$\omega^s_{(k,1,\mu)} \triangleq \hat{\delta}^{s\top} P^s_\pi(k) P^s_e \hat{e}^s_\mu, \quad \omega^s_{(k,0,\mu)} \triangleq \left(\mathbf{1} - \hat{\delta}^s\right)^\top P^s_\pi(k) P^s_e \hat{e}^s_\mu. \tag{35}$$

Corollary 6. *Under Assumption 5, for $\beta \in \{0,1\}$,*

$$\lim_{k\to\infty} \omega^s_{(k,\beta,\mu)} = \omega^s_{(\infty,\beta,\mu)}, \tag{36}$$

whose expression is (35) having ∞ instead of k.

Proof. It is a direct consequence of Assumption 5.

The Markov chain $\{\eta^s_k\}$ is fully characterized by its states (30), transition probabilities (31), and state probabilities (34), which determine the expressions for the optimal prediction and correction gains, as detailed next.

4.3. Optimal state estimation in a finite horizon

The following theorem fully characterizes the optimal SE in the finite-horizon case introduced in Section 4.1.

Theorem 1. *Under Assumptions 1–4 and the information set (16b)–(16c), the optimal SE for a system (8)–(15) with communication links described by (1)–(6) that satisfies (23)–(26) is as follows.*

$$\hat{G}_{(k,\hat{s}^s_\mu)} = -\bar{Y}_{(k,1,\mu)} C^\top \left(C \bar{Y}_{(k,1,\mu)} C^\top + \omega^s_{(k,1,\mu)} \Sigma_v \right)^{-1}, \tag{37}$$

$$G_{(k,\hat{s}^s_\mu)} = A \hat{G}_{(k,\hat{s}^s_\mu)}, \tag{38}$$

and $\bar{Y}_{(k,1,\mu)}$ is the solution to the coupled Riccati difference equations (CRDEs) for filtering, as defined below.

$$Y_{(k,0,\mu)} = A \bar{Y}_{(k,0,\mu)} A^\top + \omega^s_{(k,0,\mu)} \Sigma_w, \quad Y_{(k,1,\mu)} = A \bar{Y}_{(k,1,\mu)} A^\top + \omega^s_{(k,1,\mu)} \Sigma_w + G_{(k,\hat{s}^s_\mu)} C \bar{Y}_{(k,1,\mu)} A^\top, \tag{39a}$$

$$\bar{Y}_{(k+1,\gamma,\nu)} = \sum_{\beta=0}^{1} \sum_{\mu=1}^{M_s} \zeta^s_{(k,\mu,\gamma,\nu)} Y_{(k,\beta,\mu)}, \ \gamma \in \{0,1\}, \tag{39b}$$

$$\bar{Y}_{(0,\beta,\mu)} = \omega^s_{(0,\beta,\mu)} \left(\mathrm{X}_0 - \mathrm{x}_0 \mathrm{x}_0^\top \right), \ \beta \in \{0,1\}. \tag{39c}$$

The associated cost is

$$\sum_{k=0}^{T} \mathbb{E}\left(\|x_k - \hat{x}_k\|^2 \right) = \sum_{k=0}^{T} \sum_{\beta=0}^{1} \sum_{\mu=1}^{M_s} \hat{Y}_{(k,\beta,\mu)}, \quad \hat{Y}_{(k,0,\mu)} = \bar{Y}_{(k,0,\mu)}, \quad \hat{Y}_{(k,1,\mu)} = \bar{Y}_{(k,1,\mu)} - \hat{G}_{(k,\hat{s}^s_\mu)} C \bar{Y}_{(k,1,\mu)}. \tag{40}$$

Proof. See Appendix F.

4.4. Optimal state estimation in an infinite horizon

In the finite-horizon setting discussed in Section 4.3, the prediction and correction gains (37) and (38) are time-varying. Optimal filtering in the infinite-horizon setting concerns convergence to a steady state. The existence of a time-invariant state estimator for an MJLS is related to the notion of MS detectability (as in [8, Definition 3], [13, Definition 3.41 and Theorem 3.9]), which, for the prediction–correction filter from Section 4.1, is defined as follows.

Definition 2 (*Mean-Square Detectability*)**.** Under (1)–(6) and Assumptions 1–5, the system (8)–(15) is MS detectable if there exists a set of steady-state prediction gains $\mathcal{G} = \{G_{(\infty,\mu)}\}_{\mu=1}^{M_s}$ such that the corresponding prediction error system (28) is MS stable.

Remark 8. For the prediction error system (28), the equilibrium points, denoted, for example, as $\tilde{x}_e$ and $\tilde{X}_e$, depend on the expected values and variances of the measurement and process noise. For white noise, the expected value is zero, so $\tilde{x}_e = 0$. Then, from (29), the expected error in the current state estimate likewise converges to zero.

The general MJLS theory [13, Sections A.1–A.3.1] states that if an MJLS system is MS detectable, as in Definition 2, then the CRDEs (37)–(39) converge to time-invariant coupled algebraic Riccati equations (CAREs) that admit a unique MS-stabilizing solution. The expressions for these CAREs are given by (37)–(39b), with ∞ replacing k.

The following theorem provides practical means for solving the CAREs above by solving a constrained optimization problem whose constraints are expressed as linear matrix inequalities (LMIs).

Theorem 2. *Suppose the system (8)–(15) with communication links described by (1)–(6) satisfies (23)–(25), and, under Assumptions 1–5 and the information set (16b)–(16c), it is MS detectable. Then, the optimal SE can be obtained from solving the following LMIs.*

$$\bar{Y}^\star_{(\infty,\beta,\mu)} = \arg\max_{\bar{Y}_{(\infty,\beta,\mu)}} \mathrm{tr}\left(\sum_{\beta=0}^{1} \sum_{\mu=1}^{M_a} \bar{Y}_{(\infty,\beta,\mu)} \right) \textit{ subject to} \tag{41a}$$

$$-Y_{(\infty,0,\mu)} + A\bar{Y}_{(\infty,0,\mu)}A^\top + \omega^s_{(\infty,0,\mu)}\Sigma_w \succeq 0, \tag{41b}$$

$$\begin{bmatrix} -Y_{(\infty,1,\mu)} + A\bar{Y}_{(\infty,1,\mu)}A^\top + \omega^s_{(\infty,1,\mu)}\Sigma_w & A\bar{Y}_{(\infty,1,\mu)}C^\top \\ C\bar{Y}_{(\infty,1,\mu)}A^\top & C\bar{Y}_{(\infty,1,\mu)}C^\top + \omega^s_{(\infty,1,\mu)}\Sigma_v \end{bmatrix} \succeq 0, \tag{41c}$$

$$-\bar{Y}_{(\infty,\gamma,\nu)} + \sum_{\beta=0}^{1}\sum_{\mu=1}^{M_s}\zeta^s_{(\infty,\mu,\gamma,\nu)}Y_{(\infty,\beta,\mu)} \succeq 0, \quad C\bar{Y}_{(\infty,1,\mu)}C^\top + \omega^s_{(\infty,1,\mu)}\Sigma_v \succ 0, \tag{41d}$$

for all $\beta,\gamma \in \{0,1\}$ *and* $\mu,\nu \in \{i\}_{i=1}^{M_s}$. *The optimal gains are*

$$\hat{G}_{(\infty,\hat{s}^s_\mu)} = -\bar{Y}^\star_{(\infty,1,\mu)}C^\top\left(C\bar{Y}^\star_{(\infty,1,\mu)}C^\top + \omega^s_{(k,1,\mu)}\Sigma_v\right)^{-1}, \tag{42}$$

$$G_{(\infty,\hat{s}^s_\mu)} = A\hat{G}_{(\infty,\mu)}. \tag{43}$$

The associated cost is

$$\liminf_{k\to\infty}\mathbb{E}\left(\|x_k - \hat{x}_k\|^2\right) = \sum_{\beta=0}^{1}\sum_{\mu=1}^{M_s}\hat{Y}^\star_{(\infty,\beta,\mu)}, \quad \hat{Y}^\star_{(\infty,0,\mu)} = \bar{Y}^\star_{(\infty,0,\mu)}, \quad \hat{Y}^\star_{(\infty,1,\mu)} = \bar{Y}^\star_{(\infty,1,\mu)} - \hat{G}^\star_{(\infty,\hat{s}^s_\mu)}C\bar{Y}^\star_{(\infty,1,\mu)}. \tag{44}$$

Proof. See Appendix G.

Remark 9. Under perfect CSI (and zero-input actuation MDC with no tentative future control inputs), the optimal SE from Theorems 1 and 2 reduces to the current estimator in [8].

Remark 10. Like the prediction–correction filter in [12] with only one state, the optimal SE from Theorems 1 and 2 simplifies to the classic Kalman filter in the ideal scenario where there are no message losses on the sensing link, i.e., for $\hat{\delta}^s = \mathbf{1}$.

Remark 11. As in the general MJLS case [13, Section A.3.1], the solution to (41) is the so-called maximal solution of the filtering CAREs. For any MJLS, the maximal solution is not necessarily stabilizing, but if a stabilizing solution exists, it is the maximal one. Thus, the standard approach to infinite-horizon state estimation is to solve (41) to obtain the maximal solution and then verify whether it stabilizes the corresponding prediction error system (28). If so, the solution is stabilizing. Otherwise, no stabilizing solution exists.

Similar to [4], we define a stability verification matrix to indicate the convergence rate of the estimation error system. For that, we need to index states in (30). For the ordered pairs $(\hat{z}_1,\hat{z}_2)$, with $\hat{z}_1 \in \{0,1\}$, and $1 \le \hat{z}_2 \le M_s \le N_s$, we can use an invertible mapping $f_s : \mathbb{Z}^2 \to \mathbb{Z}^+$,

$$f_s(\hat{z}_1,\hat{z}_2) = \hat{z}_1 M_s + \hat{z}_2. \tag{45}$$

For any $\mathrm{i},\mathrm{j} \in \mathbb{Z}^+$ with $\mathrm{i},\mathrm{j} \le 2M_s$, $(\beta,\hat{s}^s_\mu)$ is indexed by i if $f_s^{-1}(\mathrm{i}) = (\beta,\mu)$ and $(\gamma,\hat{s}^s_\nu)$ is indexed by j if $f_s^{-1}(\mathrm{j}) = (\gamma,\nu)$. For notational convenience, we use the following representation of the transition probabilities in (32). For all $\beta \in \{0,1\}$,

$$\zeta^s_{(k,\mathrm{i},\mathrm{j})} = \zeta^s_{(k,\mu,\gamma,\nu)} \text{ such that } f_s^{-1}(\mathrm{i}) = (\beta,\mu), \text{ and } f_s^{-1}(\mathrm{j}) = (\gamma,\nu). \tag{46}$$

If $f_s(\beta,\mu) = \mathrm{i}$ and $f_s(\gamma,\nu) = \mathrm{j}$, then, by Corollary 3, $\zeta^s_{(\infty,\mathrm{i},\mathrm{j})} = \zeta^s_{(\infty,\mu,\gamma,\nu)}$. For $f_s^{-1}(\mathrm{i}) = (\beta,\mu)$ and $f_s^{-1}(\mathrm{j}) = (\gamma,\nu)$, let

$$\mathcal{M}_s \triangleq \left[\zeta^s_{(\infty,\mathrm{i},\mathrm{j})}\right]_{\mathrm{i},\mathrm{j}=1}^{\mathrm{L}_s}, \quad \mathrm{L}_s \triangleq 2M_s, \quad \mathcal{L}^s_{\mathrm{i}} \triangleq A + \beta G_{(\infty,\mu)}C. \tag{47}$$

$$\Lambda_s \triangleq \left(\mathcal{M}_s^\top \otimes I_{n_x^2}\right)\left(\bigoplus_{\mathrm{i}=1}^{\mathrm{L}_s}\left(\mathcal{L}^s_{\mathrm{i}} \otimes \mathcal{L}^s_{\mathrm{i}}\right)\right). \tag{48}$$

Proposition 4. *The system (8)–(15), with communication links described by (1)–(6), that satisfies (23)–(25) in the infinite-horizon setting, is MS detectable with a set of prediction gains* $\{G_{(\infty,\hat{s}^s_\mu)}\}_{\mu=1}^{M_s}$ *if and only if* $\rho(\Lambda_s) < 1$.

Proof. See Appendix H.

5. State-feedback controller

The LQR for the system described by (8) and (12)–(15) was developed in [5] and is summarized below. It is a key component of the optimal output-feedback control solution presented in Section 6.

In the state-feedback setting, $\hat{x}_k = x_k$. From (12), the control messages transmitted to the actuators are

$$\hat{u}_k = \hat{K}_{(k,\hat{\theta}^a_{k-1})}\, x_k, \quad \hat{K}^\top_{(k,\hat{\theta}^a_{k-1})} = \left[K^\top_{(k+f,\hat{\theta}^a_{k-1})}\right]_{f=0}^{n_f}. \tag{49}$$

The closed-loop system is an MJLS with a distinctive and practical representation at the time instances when actuators successfully receive messages from controllers. We denote by $\mathcal{T}$ the set of these time instances.

$$\mathcal{T} \triangleq \left\{k : \delta^a_k = 1\right\}_{k\in\mathbb{Z}^{0+}} = \{\tau_{(m)}\}_{m\in\mathbb{Z}^{0+}}, \tag{50}$$

These time instances are separated by consecutive actuation message dropouts governed by the actuation FSMC (1)–(6), with $\lambda = a$. We define the number of consecutive actuation message dropouts that the controller knows, based on the information set $\mathcal{I}^{lqr}_k$ in (16a), as a stochastic variable Δ_k:

$$\Delta_k \triangleq (1-\delta^a_{k-1})(\Delta_{k-1}+1). \tag{51}$$

$$\tau_{(m+1)} = \tau_{(m)} + 1 + \Delta_{\tau_{(m+1)}}. \tag{52}$$

For the notational convenience, for any $k, h \in \mathbb{Z}^{0+}$, we let

$$\Psi_{(h)} \triangleq \sum_{i=0}^{h} A^{h-i} B F H^i,\ W_{(k,h)} \triangleq \sum_{i=0}^{h} A^{h-i} w_{k+i}. \tag{53}$$

Finally, we group the current duration of the actuation message error burst and the last observed CSI for the actuation link in an augmented discrete state

$$\eta^a_k \triangleq (\Delta_k, \hat{\theta}^a_{k-1}). \tag{54}$$

From [5, Proposition 1 and Remark 1], the system described by (8), (12)–(15), and (1)–(6) is trace-equivalent to

$$\begin{cases} \Delta_{\tau_{(m+1)}} = n \in \mathbb{Z}^{0+} \Rightarrow \forall h \in \mathbb{Z}^{0+} : h \le n, \\ x_{\tau_{(m)}+1+h} = \left(A^{h+1} + \Psi_{(h)} \hat{K}_{(\tau_{(m)},\hat{\theta}^a_{\tau_{(m)}-1})}\right) x_{\tau_{(m)}} + W_{(\tau_{(m)},h)}, \end{cases} \tag{55}$$

with the trace equivalence meaning that for any given initial system state x_0, the control law that satisfies (19) and (49), and the realization of $\left(\delta^a_t\right)_{t=0}^{\tau_m+n}$ and $\left(w_t\right)_{t=0}^{\tau_m+n}$, the states $x_{\tau_{(m)}}$ and $x_{\tau_{(m)}+1+h}$ obtained from (8) and (55) will be the same $\forall h \in \mathbb{Z}^{0+}$ such that $h \le n$. To the controller, $\eta^a_{\tau_{(m)}}$ is known, while $\eta^a_{\tau_{(m+1)}}$ is a random variable. From [5, Theorem 1],

$$\mathbb{P}\left(\eta^a_{\tau_{(m+1)}} = (n, \hat{s}^a_\nu) \mid \eta^a_{\tau_{(m)}} = (\ell, \hat{s}^a_\mu)\right) = \frac{\hat{e}^{a\top}_\mu P^{a\top}_e P^{a\top}_\pi (\tau_{(m)}-1) P^a_s (P^a_f)^n P^a_\alpha(\nu) P^a_s \mathbf{1}}{\hat{e}^{a\top}_\mu P^{a\top}_e P^{a\top}_\pi (\tau_{(m)}-1) P^a_s \mathbf{1}}. \tag{56}$$

We note that the transition probabilities in (56) are independent of ℓ. Thus, for notational convenience, we denote the expressions for the transition probabilities in (56) as follows.

$$\zeta^a_{(\tau_{(m)},\mu,n,\nu)} \triangleq \frac{\hat{e}^{a\top}_\mu P^{a\top}_e P^{a\top}_\pi (\tau_{(m)}-1) P^a_s (P^a_f)^n P^a_\alpha(\nu) P^a_s \mathbf{1}}{\hat{e}^{a\top}_\mu P^{a\top}_e P^{a\top}_\pi (\tau_{(m)}-1) P^a_s \mathbf{1}}. \tag{57}$$

For an arbitrarily small threshold ϵ, we define a maximal number of consecutive actuation message dropouts as

$$L \triangleq \arg\min_{\hat{n}\in\mathbb{Z}^+} \zeta^a_{(\tau_{(m)},\mu,\hat{n},\nu)} < \epsilon, \tag{58}$$

which, by [5, Proposition 2], always exists.

With (49)–(58), we have all the ingredients needed to present the optimal state-feedback controllers.

5.1. LQR in a finite horizon

From [5, Theorem 2], the solution to Problem 1 in the state-feedback setting ($y_k = x_k \Rightarrow \hat{x}_k = x_k\ \forall k$) is (59)–(67).

$$\hat{K}_{(k,\hat{s}^a_\mu)} = -\mathcal{B}^{-1}_{(k,\mu)} \mathcal{C}_{(k,\mu)}. \tag{59}$$

$$\mathcal{A}_{(k,\mu)} = Q + \sum_{h=0}^{L-\xi_k} \sum_{\nu=1}^{M_a} \zeta^a_{(k,\mu,h,\nu)} \left((A^{h+1})^\top \mathcal{X}_{(k+1+h,\nu)} A^{h+1} + \sum_{r=1}^{h} A^{r\top} Q A^r\right), \tag{60}$$

$$\mathcal{B}_{(k,\mu)} = F^\top R F + \sum_{h=0}^{L-\xi_k} \sum_{\nu=1}^{M_a} \zeta^a_{(k,\mu,h,\nu)} \left(\Psi^\top_{(h)} \mathcal{X}_{(k+1+h,\nu)} \Psi_{(h)} + \sum_{r=1}^{h} \left(\Psi^\top_{(r-1)} Q \Psi_{(r-1)} + H^{r\top} F^\top R F H^r\right)\right), \tag{61}$$

$$\mathcal{C}_{(k,\mu)} = \sum_{h=0}^{L-\xi_k} \sum_{\nu=1}^{M_a} \zeta^a_{(k,\mu,h,\nu)} \left(\Psi^\top_{(h)} \mathcal{X}_{(k+1+h,\nu)} A^{h+1} + \sum_{r=1}^{h} \Psi^\top_{(r-1)} Q A^r\right), \tag{62}$$

$$\mathcal{X}_{(k,\mu)} = \mathcal{A}_{(k,\mu)} - C_{(k,\mu)}^{\top} B_{(k,\mu)}^{-1} C_{(k,\mu)}. \tag{63}$$

$$g_{(k,\mu)} = \sum_{h=0}^{L-\xi_k} \sum_{\nu=1}^{M_a} \zeta_{(k,\mu,h,\nu)}^{a} \left(g_{(k+1+h,\nu)} + \sum_{t=0}^{h} \operatorname{tr}(A^{t\top} \mathcal{X}_{(k+1+h,\nu)} A^{t} \Sigma_W) + \sum_{r=1}^{h} \sum_{\iota=0}^{r-1} \operatorname{tr}(A^{t\top} Q A^{t} \Sigma_W) \right). \tag{64}$$

$$\mathcal{X}_{(T,\mu)} = Q, \; g_{(T,\mu)} = 0. \tag{65}$$

$$\xi_k \triangleq \max\{0, k+1+L-T\} \tag{66}$$

so that $\xi_{T-1} = L$, and $\xi_k = 0 \; \forall k < T - L$. The optimal cost is

$$J_T^{\star}(x_0) = x_0^{\top} \left(\sum_{\mu=1}^{M_a} \mathcal{X}_{(0,\mu)} \vartheta_{\mu}^{a} \right) x_0 + \sum_{\mu=1}^{M_a} g_{(0,\mu)} \vartheta_{\mu}^{a}, \quad \vartheta_{\mu}^{a} = \sum_{i=1}^{N_a} \alpha_{i\mu}^{a} \pi_i^{a}(0). \tag{67}$$

5.2. LQR in an infinite horizon

An infinite-horizon LQR aims to ensure that the system's state converges to an equilibrium point. This is possible only for stabilizable systems, formally defined as follows [5, Definition 1].

Definition 3 (*Mean-Square Stabilizability*)**.** Under (1)–(6) and Assumptions 1–5, the system described by (8) and (13)–(15) is MS stabilizable by a state-feedback controller with one-step delayed access to the CSI measurements if, for any initial condition (x_0, θ_0^a) and each detected CSI $\hat{s}_{\mu}^{a}$, there exists a gain $\hat{K}_{(\infty,\hat{s}_{\mu}^{a})}$ such that $\hat{u}_k = \hat{K}_{(\infty,\hat{\theta}_{k-1})} x_k$ is a stabilizing actuation message.

To present the MS stabilizability conditions and the infinite-horizon LQR, let $\hat{K}_{(\infty,\hat{\theta}_{k-1}^{a})}$ denote the time-invariant version of (49),

$$\hat{K}_{(\infty,\hat{\theta}_{k-1}^{a})}^{\top} = \left[K_{(f,\hat{\theta}_{k-1}^{a})}^{\top} \right]_{f=0}^{n_f} \forall k. \tag{68}$$

As detailed in [4,5], MS stability analysis requires accounting for each control message transmission outcome as perceived by the actuators. Thus, we consider the following augmented discrete states.

$$\hat{\varphi}_{\tau_{(m+1)}} = (\hat{\theta}_{\tau_{(m+1)}}^{a}, \Delta_{\tau_{(m+1)}}, \hat{\theta}_{\tau_{(m)}-1}^{a}). \tag{69}$$

By [5, Theorem 3], the transition probabilities between consecutive states are given by

$$\mathbb{P}(\hat{\varphi}_{\tau_{(m+2)}} = (\hat{s}_{\nu_1}^{a}, n, \hat{s}_{\nu_0}^{a}) \mid \hat{\varphi}_{\tau_{(m+1)}} = (\hat{s}_{\mu_1}^{a}, \ell, \hat{s}_{\mu_0}^{a})) = \frac{\hat{e}_{\mu_0}^{a\top} P_e^{a\top} P_{\pi}^{a}(\tau_{(m)}-1) P_s^{a} (P_f^{a})^{\ell} P_{\alpha}^{a}(\nu_0) P_s^{a} P_{\alpha}^{a}(\mu_1) (P_f^{a})^{n} P_s^{a} P_e^{a} \hat{e}_{\nu_1}^{a}}{\hat{e}_{\mu_0}^{a\top} P_e^{a\top} P_{\pi}^{a}(\tau_{(m)}-1) P_s^{a} (P_f^{a})^{\ell} P_s^{a} P_e^{a} \hat{e}_{\mu_1}^{a}}. \tag{70}$$

To concisely refer to these states and the transition probabilities among them, we index the values of the ordered triples (z_1, z_2, z_3) with $1 \le z_1, z_3 \le M_a \le N_a$ and $0 \le z_2 \le L$ using an invertible mapping $f_a : \mathbb{Z}^3 \to \mathbb{Z}^+$,

$$f_a(z_1, z_2, z_3) = z_2 M_a^2 + (z_3 - 1) M_a + z_1. \tag{71}$$

For any $\mathrm{i}, \mathrm{j} \in \mathbb{Z}^+$ with $\mathrm{i}, \mathrm{j} \le (L+1) M_a^2$, $(\hat{s}_{\mu_1}^{a}, \ell, \hat{s}_{\mu_0}^{a})$ is indexed by i if $f_a^{-1}(\mathrm{i}) = (\mu_1, \ell, \mu_0)$ and $(\hat{s}_{\nu_1}^{a}, n, \hat{s}_{\nu_0}^{a})$ is indexed by j if $f_a^{-1}(\mathrm{j}) = (\nu_1, n, \nu_0)$. Furthermore, for notational convenience, we use the following compact representation of the transition probabilities in (70). If $f_a(\mu_1, \ell, \mu_0) = \mathrm{i}$ and $f_a(\nu_1, n, \nu_0) = \mathrm{j}$, then

$$\varrho_{\mathrm{ij}}(\tau_{(m)}-1) \triangleq \frac{\hat{e}_{\mu_0}^{a\top} P_e^{a\top} P_{\pi}^{a}(\tau_{(m)}-1) P_s^{a} (P_f^{a})^{\ell} P_{\alpha}^{a}(\nu_0) P_s^{a} P_{\alpha}^{a}(\mu_1) (P_f^{a})^{n} P_s^{a} P_e^{a} \hat{e}_{\nu_1}^{a}}{\hat{e}_{\mu_0}^{a\top} P_e^{a\top} P_{\pi}^{a}(\tau_{(m)}-1) P_s^{a} (P_f^{a})^{\ell} P_s^{a} P_e^{a} \hat{e}_{\mu_1}^{a}}. \tag{72}$$

Under Assumption 5,

$$\lim_{\tau_{(m)} \to \infty} \varrho_{\mathrm{ij}}(\tau_{(m)} - 1) = \varrho_{\mathrm{ij}}(\infty), \tag{73}$$

whose expression is (72) having ∞ instead of $\tau_{(m)}-1$. For $f_a^{-1}(\mathrm{i}) = (\mu_1, \ell, \mu_0)$ and $f_a^{-1}(\mathrm{j}) = (\nu_1, n, \nu_0)$, let

$$\mathcal{M}_a \triangleq \left[\varrho_{\mathrm{ij}}(\infty) \right]_{\mathrm{i},\mathrm{j}=1}^{\mathrm{L}_a}, \quad \mathrm{L}_a \triangleq (L+1) M_a^2, \quad \mathcal{L}_{\mathrm{j}}^{a} \triangleq A^{n+1} + \Psi_{(n)} \hat{K}_{(\infty,\hat{s}_{\nu_0}^{a})}^{\star}, \quad \Lambda_a \triangleq \left(\bigoplus_{\mathrm{j}=1}^{\mathrm{L}_a} \left(\mathcal{L}_{\mathrm{j}}^{a} \otimes \mathcal{L}_{\mathrm{j}}^{a} \right) \right) \left(\mathcal{M}_a^{\top} \otimes I_{n_x^2} \right). \tag{74}$$

By [5, Theorem 4], the system (8), (13)–(15), with the actuation communication link described by (1)–(6), and the time-invariant version of (49) given by (68), under Assumptions 1–5, is MS stable if and only if $\rho(\Lambda_a) < 1$.

If the system is MS stabilizable according to Definition 3, then, by [5, Theorem 5], the optimal gains can be obtained as follows.

$$\hat{K}_{(\infty,\hat{s}_{\mu}^{a})} = -\hat{B}_{(\infty,\mu)}^{-1} \hat{C}_{(\infty,\mu)}, \tag{75}$$

where $\hat{\mathcal{B}}_{(\infty,\mu)}$ and $\hat{\mathcal{C}}_{(\infty,\mu)}$ are defined by (61) and (62) for $k=\infty$, and $\mathcal{X}_{(\infty,\mu)}$ is the solution of the following LMIs.

$$\hat{\mathcal{X}}_{(\infty,\mu)} = \arg\max_{\mathcal{X}_{(\infty,\mu)}} \operatorname{tr}\left(\sum_{\mu=1}^{M_a} \mathcal{X}_{(\infty,\mu)}\right) \text{ subject to} \tag{76a}$$

$$\begin{bmatrix} -\mathcal{X}_{(\infty,\mu)} + \mathcal{A}_{(\infty,\mu)} & \mathcal{C}_{(\infty,\mu)}^{\top} \\ \mathcal{C}_{(\infty,\mu)} & \mathcal{B}_{(\infty,\mu)} \end{bmatrix} \succeq 0, \quad \mathcal{X}_{(\infty,\mu)} \succeq 0, \quad \mathcal{B}_{(\infty,\mu)} \succ 0, \tag{76b}$$

with the terms in (76) defined by (60)–(63) for $k=\infty$, where $\xi_\infty = 0$, and $\zeta^a_{(\infty,\mu,h,\nu)} = \lim_{\tau_{(m)}\to\infty} \zeta^a_{(\tau_{(m)},\mu,h,\nu)}$, expressed by (57) having ∞ instead of $\tau_{(m)}-1$.

The optimal cost that minimizes (21) is (77), where $\psi^a_{(h,\nu)}$ are the elements of the steady-state distribution of $\{\eta^a_{\tau_{(m)}}\}$:

$$\sum_{\mu=1}^{M_a} \sum_{\ell\in\mathbb{Z}^{0+}} \psi^a_{(\ell,\mu)} \zeta^a_{(\infty,\mu,n,\nu)} = \psi^a_{(n,\nu)}, \quad \sum_{\mu=1}^{M_a} \sum_{\ell\in\mathbb{Z}^{0+}} \psi^a_{(\ell,\mu)} = 1.$$

$$J^\star_\infty = \sum_{h=0}^{L} \sum_{\nu=1}^{M_a} \psi^a_{(h,\nu)} \left(\sum_{r=1}^{h} \sum_{\imath=0}^{r-1} \operatorname{tr}(A^{\imath\top} Q A^\imath \Sigma_W) + \sum_{t=0}^{h} \operatorname{tr}(A^{t\top} \hat{\mathcal{X}}_{(\hat{s}_\nu)} A^t \Sigma_W) \right). \tag{77}$$

6. Separation principle

This section presents the structure of the complete output-feedback controller and demonstrates the validity of the separation principle discussed in Section 3.5.

Consider an arbitrary discrete time point k before the first successful actuation message transmission or between two successful actuation message deliveries, as defined in (50): $k\in\mathbb{Z}^{0+}$ and $k<\tau_{(0)}$ or $k\geq\tau_{(m)}$ and $k<\tau_{(m+1)}$, for all $m\in\mathbb{Z}^{0+}$. By (52), there is $h\in\mathbb{Z}^{0+}$ such that $k=h$ if $k<\tau_{(0)}$ and $h\leq\Delta_{(0)}$ or $k=\tau_{(m)}+h$ if $k<\tau_{(m+1)}$ and $h\leq\Delta_{\tau_{(m+1)}}$. This h is the number of consecutive actuation message dropouts in k. Consider the optimal SE from Theorems 1 or 2 as input to the optimal state-feedback controller, with gains described by (59) or (75). By (8)–(15) and (23)–(26), the complete output-feedback controller has the following structure.

$$\begin{cases} \bar{x}_0 = x_0, \\ \hat{x}_k = \bar{x}_k - \hat{G}_{(k,\hat{\theta}^s_k)} \left(\hat{y}_k - \delta^s_k C \bar{x}_k\right), \\ \hat{u}_k = \hat{K}_{(k,\hat{\theta}^a_{k-1})} \hat{x}_k, \\ \bar{x}_{k+1} = A\bar{x}_k + BFH^h \hat{K}_{(\tau_{(m)},\hat{\theta}^a_{\tau_{(m)}-1})} \hat{x}_{\tau_{(m)}} - G_{(k,\hat{\theta}^s_k)} \left(\hat{y}_k - \delta^s_k C \bar{x}_k\right), \end{cases} \tag{78}$$

where $\tau_{(m)}$ should be substituted by 0 if $k<\tau_{(0)}$ and, by convention, $\hat{\theta}^a_{-1} = \hat{\theta}^a_0$. Notice that $h=0$ implies $k=\tau_{(m)}$. The infinite-horizon version uses $\hat{G}_{(\infty,\hat{\theta}^s_k)}$, $G_{(\infty,\hat{\theta}^s_k)}$, $\hat{K}_{(\infty,\hat{\theta}^a_{k-1})}$, and $\hat{K}_{(\infty,\hat{\theta}^a_{\tau_{(m)}-1})}$ instead of $\hat{G}_{(k,\hat{\theta}^s_k)}$, $G_{(k,\hat{\theta}^s_k)}$, $\hat{K}_{(k,\hat{\theta}^a_{k-1})}$, and $\hat{K}_{(\tau_{(m)},\hat{\theta}^a_{\tau_{(m)}-1})}$.

The dynamics of the closed-loop system can be described as follows. For $k=\tau_{(m)}+h$, with $h\in\mathbb{Z}^{0+}$ and $h\leq\Delta_{\tau_{(m+1)}}$,

$$x_{k+1} = Ax_k + BFH^h \hat{K}_{(\tau_{(m)},\hat{\theta}^a_{\tau_{(m)}-1})} \hat{x}_{\tau_{(m)}} + w_k \tag{79}$$

From (10), (11), (15), (27), (78), and (79),

$$\tilde{x}_{k+1} = \left(A + \delta^s_k G_{(k,\hat{\theta}^s_k)} C\right) \tilde{x}_k + \delta^s_k G_{(k,\hat{\theta}^s_k)} v_k + w_k. \tag{80}$$

Notice that (80) is (28) evaluated at the time points $k+1$ and k rather than k and $k-1$. Furthermore, the expression of the error in the current state estimate at time k is given by (29). Therefore, for $h=0$, that is for $k=\tau_{(m)}$,

$$\hat{x}_{\tau_{(m)}} = x_{\tau_{(m)}} - \left(I_{n_x} + \delta^s_{\tau_{(m)}} \hat{G}_{(\tau_{(m)},\hat{\theta}^s_{\tau_{(m)}})} C\right) \tilde{x}_{\tau_{(m)}} - \delta^s_{\tau_{(m)}} \hat{G}_{(\tau_{(m)},\hat{\theta}^s_{\tau_{(m)}})} v_{\tau_{(m)}}. \tag{81}$$

For notational convenience, let

$$Y_{(\eta^s_k)} \triangleq \begin{cases} \delta^s_k \hat{G}_{(k,\hat{\theta}^s_k)} & \text{in the finite-horizon setting,} \\ \delta^s_k \hat{G}_{(\infty,\hat{\theta}^s_k)} & \text{in the infinite-horizon setting.} \end{cases} \tag{82}$$

By (55), with (12) instead of (49), and (81) and (82), for $k=\tau_{(m)}+h$, with $h\in\mathbb{Z}^{0+}$ and $h\leq\Delta_{\tau_{(m+1)}}$, (79) becomes

$$x_{k+1} = \left(A^{h+1} + \Psi_{(h)} \hat{K}_{(\tau_{(m)},\hat{\theta}^a_{\tau_{(m)}-1})}\right) x_{\tau_{(m)}} + W_{(\tau_{(m)},h)} - \Psi_{(h)} \hat{K}_{(\tau_{(m)},\hat{\theta}^a_{\tau_{(m)}-1})} \left(\left(I_{n_x} + Y_{(\eta^s_{\tau_{(m)}})} C\right) \tilde{x}_{\tau_{(m)}} + Y_{(\eta^s_{\tau_{(m)}})} v_{\tau_{(m)}}\right). \tag{83}$$

From (38), (43), (80), and (82),

$$\tilde{x}_{k+1} = \left(\prod_{i=0}^{h} A \left(I_{n_x} + Y_{(\eta^s_{\tau_{(m)}+h-i})} C\right)\right) \tilde{x}_{\tau_{(m)}} + \sum_{i=0}^{h} \left(\prod_{j=i+1}^{h} A \left(I_{n_x} + Y_{(\eta^s_{\tau_{(m)}+h-j+1})} C\right)\right) \left(A Y_{(\eta^s_{\tau_{(m)}+i})} v_{\tau_{(m)}+i} + w_{\tau_{(m)}+i}\right). \tag{84}$$

By (83) and (84), the closed-loop dynamics can be expressed in the following compact form. Let

$$\left(\vec{w}^{\,k}_{\tau_{(m)}}\right)^{\top} \triangleq \left[w^{\top}_{\tau_{(m)+i}}\right]_{i=0}^{h}, \quad \left(\vec{v}^{\,k}_{\tau_{(m)}}\right)^{\top} \triangleq \left[v^{\top}_{\tau_{(m)+i}}\right]_{i=0}^{h}, \quad \mathcal{D}_0 \triangleq [0]_{i=1}^{h}, \quad \mathcal{D}_1(h) \triangleq \left[A^{h-i}\right]_{i=0}^{h}, \tag{85a}$$

$$\mathcal{D}_2(h, \hat{\theta}^{a}_{\tau_{(m)}-1}, \eta^{s}_{\tau_{(m)}}) \triangleq \left[-\Psi_{(h)}\hat{K}_{(\tau_{(m)},\hat{\theta}^{a}_{\tau_{(m)}-1})}Y_{(\eta^{s}_{\tau_{(m)}})} \quad \mathcal{D}_0\right], \quad \mathcal{D}_3(h, \eta^{s}_{\tau_{(m)}}) \triangleq \left[\prod_{j=i+1}^{h} A\left(I_{n_x} + Y_{(\eta^{s}_{\tau_{(m)}+h-j+1})}C\right)\right]_{i=0}^{h}, \tag{85b}$$

$$\mathcal{D}_4(h, \eta^{s}_{\tau_{(m)}}) \triangleq \left[\left(\prod_{j=i+1}^{h} A\left(I_{n_x} + Y_{(\eta^{s}_{\tau_{(m)}+h-j+1})}C\right)\right)AY_{(\eta^{s}_{\tau_{(m)}+i})}\right]_{i=0}^{h}, \tag{85c}$$

$$\mathcal{E}(h, \hat{\theta}^{a}_{\tau_{(m)}-1}, \eta^{s}_{\tau_{(m)}}) \triangleq \begin{bmatrix} A^{h+1} + \Psi_{(h)}\hat{K}_{(\tau_{(m)},\hat{\theta}^{a}_{\tau_{(m)}-1})} & -\Psi_{(h)}\hat{K}_{(\tau_{(m)},\hat{\theta}^{a}_{\tau_{(m)}-1})}\left(I_{n_x} + Y_{(\eta^{s}_{\tau_{(m)}})}C\right) \\ 0 & \prod_{i=0}^{h} A\left(I_{n_x} + Y_{(\eta^{s}_{\tau_{(m)}+h-i})}C\right) \end{bmatrix}. \tag{85d}$$

$$\begin{bmatrix} x_{k+1} \\ \tilde{x}_{k+1} \end{bmatrix} = \mathcal{E}(h, \hat{\theta}^{a}_{\tau_{(m)}-1}, \eta^{s}_{\tau_{(m)}}) \begin{bmatrix} x_{\tau_{(m)}} \\ \tilde{x}_{\tau_{(m)}} \end{bmatrix} + \begin{bmatrix} \mathcal{D}_1(h) & \mathcal{D}_2(h, \hat{\theta}^{a}_{\tau_{(m)}-1}, \eta^{s}_{\tau_{(m)}}) \\ \mathcal{D}_3(h, \eta^{s}_{\tau_{(m)}}) & \mathcal{D}_4(h, \eta^{s}_{\tau_{(m)}}) \end{bmatrix} \begin{bmatrix} \vec{w}^{\,k}_{\tau_{(m)}} \\ \vec{v}^{\,k}_{\tau_{(m)}} \end{bmatrix}. \tag{86}$$

Notice that $\mathcal{E}(h, \hat{\theta}^{a}_{\tau_{(m)}-1}, \eta^{s}_{\tau_{(m)}})$ in (85d) is an upper-triangular block-diagonal matrix, indicating that the SE's prediction-error dynamics (driven by η^{s}_{k}) are independent of the system's state dynamics (induced by η^{a}_{k}). Thus, the optimal SE and LQR can be designed separately, with the overall optimal cost being the sum of the optimal costs for estimation and control, as given by (40) or (44) and (67) or (77). Intuitively, because state estimation is not affected by the control input, the additional cost arises from the error in the current corrected state estimate, which is exactly the source of the estimation cost. We refer the reader to [13, Chapter 6] for additional technical details on the separation principle and the derivation of the related optimal cost for the general MJLS with dynamics governed by a single perfectly observable Markov chain.

7. Numerical example

We consider a linearized model of a rotary inverted pendulum described in [4,5], and the references therein. The system state comprises the rotary arm and pendulum angles and their derivatives, i.e., the corresponding angular velocities. Linearization about the unstable equilibrium point, together with zero-order hold discretization at a sampling rate of 12 Hz, yields the following discrete-time system matrices.

$$A = \begin{bmatrix} 1 & 0.224 & 0.055 & 0.004 \\ 0 & 1.369 & -0.028 & 0.090 \\ 0 & 4.994 & 0.391 & 0.167 \\ 0 & 8.618 & -0.634 & 1.270 \end{bmatrix}, \quad B = \begin{bmatrix} 0.227 \\ 0.218 \\ 4.944 \\ 4.820 \end{bmatrix}, \quad C = \begin{bmatrix} 1 & 0 & 0 & 0 \\ 0 & 1 & 0 & 0 \end{bmatrix}. \tag{87}$$

The system state is perturbed by additive white Gaussian process noise with covariance matrix $\Sigma_w = 4 \cdot 10^{-6} I_4$. The measurements are corrupted by additive white Gaussian measurement noise with covariance matrix $\Sigma_v = 4 \cdot 10^{-6} I_2$. The state- and input-weighting matrices are $Q = \bigoplus\{1, 5, 1, 1\}$ and $R = 10$. The controller aims to stabilize the pendulum in an upright position (inverted pendulum angle of zero) while minimizing the associated costs. We set $n_f = 1$ to allow the controller to compute and send one tentative future control input, which significantly improves stability and reduces control costs compared with $n_f = 0$ in the state-feedback setting analyzed in [5]. Furthermore, we set $\Phi = 0.921$, a significant parameter from [4], because it provides the most stable closed-loop behavior in the mean-square sense in the state-feedback setting under perfect CSI.

We use the same four-state Markov channel model from [5] for the actuation and sensing links and focus on a scenario of partial observability of the FSMC states, with the first two channel states in the first cluster and the remaining two in the second cluster. Formally, for $\lambda = \{s, a\}$

$$P_c^{\lambda} = \begin{bmatrix} 0.257 & 0.027 & 0.032 & 0.684 \\ 0.182 & 0.023 & 0.028 & 0.767 \\ 0.172 & 0.022 & 0.027 & 0.779 \\ 0.058 & 0.010 & 0.012 & 0.920 \end{bmatrix}, \quad \hat{\delta}^{\lambda} = \begin{bmatrix} 0.026 \\ 0.375 \\ 0.634 \\ 0.995 \end{bmatrix}, \quad P_e^{\lambda} = \begin{bmatrix} 1 & 0 \\ 1 & 0 \\ 0 & 1 \\ 0 & 1 \end{bmatrix}. \tag{88}$$

The optimal infinite-horizon correction and prediction gains (42) and (43) in Theorem 2 are as follows.

$$\hat{G}_{(\infty,1)} = \begin{bmatrix} -1 & 0 \\ 0 & -1 \\ 0 & 0 \\ 0 & 0 \end{bmatrix}, \quad \hat{G}_{(\infty,2)} = \begin{bmatrix} -0.748 & -0.014 \\ -0.014 & -0.923 \\ -0.636 & -2.370 \\ 0.167 & -9.291 \end{bmatrix}, \quad G_{(\infty,1)} = \begin{bmatrix} -1 & -0.224 \\ 0 & -1.369 \\ 0 & -4.994 \\ 0 & -8.618 \end{bmatrix}, \quad G_{(\infty,2)} = \begin{bmatrix} -0.785 & -0.388 \\ 0.014 & -2.033 \\ -0.290 & -7.086 \\ 0.496 & -18.248 \end{bmatrix}$$

The corresponding optimal SE cost in (44) is 43404224.451. We observe that using $\bar{Y}^{\star}_{(\infty,\beta,\mu)}$ instead of $\hat{Y}^{\star}_{(\infty,0,\mu)}$ yields the optimal prediction error cost of 86808413.533. This shows that performing the correction step halves the optimal SE cost compared with relying exclusively on the prediction step in the setting considered in this numerical example.

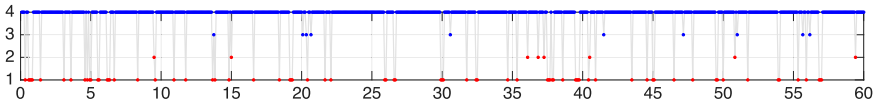

Fig. 5. Hidden state of the sensing link over 60 s of 12 Hz communication.

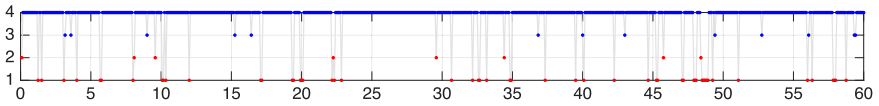

Fig. 6. Hidden state of the actuation link over 60 s of 12 Hz communication.

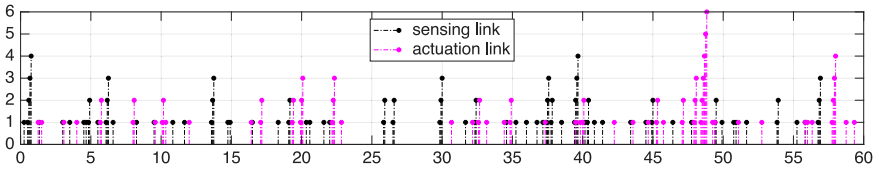

Fig. 7. The number of consecutive message dropouts on sensing and actuation links over 60 s of 12 Hz communication.

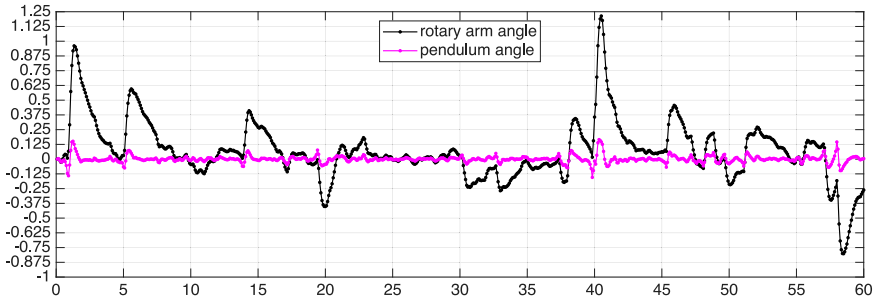

Fig. 8. The closed-loop system state dynamics.

The optimal LQR gain in (75) is given by

$$\hat{K}_{(\infty,1)} = \begin{bmatrix} 0.081 & -4.085 & 0.278 & -0.476 \\ -0.088 & -0.457 & -0.008 & -0.015 \end{bmatrix}, \quad \hat{K}_{(\infty,2)} = \begin{bmatrix} 0.081 & -4.080 & 0.277 & -0.475 \\ -0.088 & -0.462 & -0.007 & -0.016 \end{bmatrix}$$

The corresponding optimal LQR cost in (77) is 275377.928. The overall optimal output-feedback cost is the sum of the SE and LQR costs, totaling 43679602.379, with the SE cost accounting for 99.37% of the total. This data underscores the key role of state estimation in output-feedback settings.

The following figures provide an illustrative example of the closed-loop system dynamics, showing stable behavior despite a significant number of consecutive message losses on both the actuation and sensing links. All traces span 60 s of 12 Hz sampling and communication.

Figs. 5 and 6 show the hidden Markov chain state evolutions for the sensing and actuation links. The EPMs in (88) provide partial CSI: the first two states of each FSMC have low successful message-delivery probabilities and belong to the first cluster (in red), whereas the remaining two states have higher successful message-delivery probabilities and belong to the second cluster (in blue). Fig. 7 shows the corresponding traces of the number of consecutive message dropouts over the sensing (in black) and actuation (in magenta) links. In this example, the actuation link has the longest message dropout burst of 6 messages. The longest observed message dropout burst on the sensing link is 4, but the link also experiences more frequent message dropout bursts of 3 or more messages.

All remaining figures present information on the first two components of the system's state, corresponding to the rotary arm angle (in black) and the pendulum angle (in magenta), both measured in radians. As shown in the system output matrix C in (87), these components are directly observed by the remote sensors. The remaining components of the system's state are omitted because they are derivatives of the first two and can thus be inferred from their traces. Fig. 8 shows the traces of the first two components of the system's state x_k, indicating stable dynamics, with the pendulum angle remaining close to the origin and the rotary arm returning to the origin after compensating for perturbations caused by process and measurement noise and message dropouts. Fig. 9 quantifies the errors in the inputs to the state estimator due to sensor message dropouts, defined as $y_k - \hat{y}_k$. Together, Figs. 8 and 9 highlight sensor message dropouts as a major disturbance. Finally, Fig. 10 shows the stable dynamics of the SE error $x_k - \hat{x}_k$.

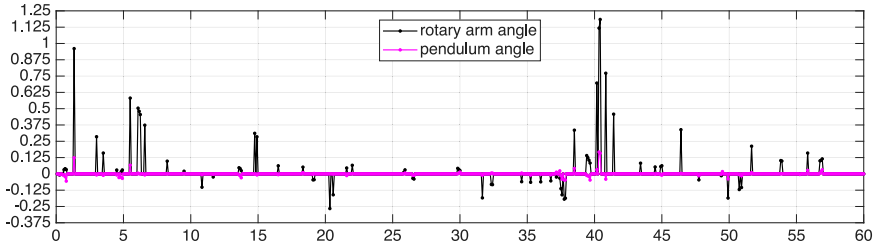

Fig. 9. The state-estimation input errors.

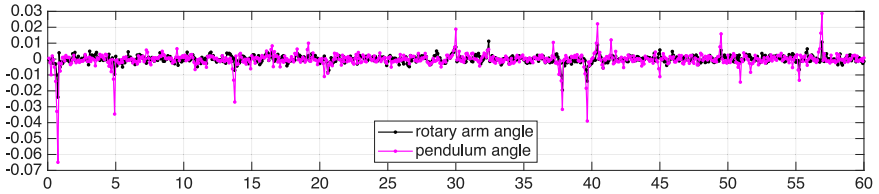

Fig. 10. The state estimation error dynamics.

8. Conclusion

This paper presented a comprehensive framework for designing optimal output-feedback controllers over wireless communication links. Future work could include addressing constrained control problems and exploring application-layer actuation acknowledgment.

CRediT authorship contribution statement

Yuriy Zacchia Lun: Writing – review & editing, Writing – original draft, Methodology, Investigation, Conceptualization. **Fortunato Santucci:** Supervision, Funding acquisition. **Alessandro D'Innocenzo:** Supervision, Methodology, Conceptualization, Funding acquisition.

Declaration of competing interest

The authors declare that they have no known competing financial interests or personal relationships that could have appeared to influence the work reported in this paper.

Appendix A. Proof of Proposition 1

Information set (16c) includes the sequences of control messages, $\left(\hat{u}_{t-1}\right)_{t=1}^{k}$, and their acknowledgments, $\left(\delta_{t-1}^{a}\right)_{t=1}^{k}$. Assumption 2 ensures knowledge of the matrices H and F. Thus, the SE can compute (23), which, by construction, equals (14). Consequently, $u_{t-1} = F\check{u}_{t-1}$, $\forall t \in \mathbb{Z}^{+}$ such that $t \leq k$. □

Appendix B. Proof of Proposition 2

We first consider the first equation in (31):

$$\mathbb{P}\left(\eta_{k+1}^{s} = (1, \hat{s}_{\nu}^{s}) \mid \eta_{k}^{s} = (\beta, \hat{s}_{\mu}^{s})\right) = \mathbb{P}\left(\delta_{k+1}^{s} = 1, \hat{\theta}_{k+1}^{s} = \hat{s}_{\nu}^{s} \mid \delta_{k}^{s} = \beta, \hat{\theta}_{k}^{s} = \hat{s}_{\mu}^{s}\right) \tag{B.1}$$

$$= \frac{\mathbb{P}\left(\delta_{k+1}^{s} = 1, \hat{\theta}_{k+1}^{s} = \hat{s}_{\nu}^{s}, \delta_{k}^{s} = \beta, \hat{\theta}_{k}^{s} = \hat{s}_{\mu}^{s}\right)}{\mathbb{P}\left(\delta_{k}^{s} = \beta, \hat{\theta}_{k}^{s} = \hat{s}_{\mu}^{s}\right)} \tag{B.2}$$

$$= \frac{\mathbb{P}\left(\delta_{k+1}^{s} = 1, \hat{\theta}_{k+1}^{s} = \hat{s}_{\nu}^{s}, \hat{\theta}_{k}^{s} = \hat{s}_{\mu}^{s}, \delta_{k}^{s} = \beta\right)}{\mathbb{P}\left(\hat{\theta}_{k}^{s} = \hat{s}_{\mu}^{s}, \delta_{k}^{s} = \beta\right)} \tag{B.3}$$

$$= \frac{\mathbb{P}\left(\delta_{k+1}^{s} = 1, \hat{\theta}_{k+1}^{s} = \hat{s}_{\nu}^{s}, \hat{\theta}_{k}^{s} = \hat{s}_{\mu}^{s}, \delta_{k}^{s} = \beta\right)}{\mathbb{P}\left(\hat{\theta}_{k}^{s} = \hat{s}_{\mu}^{s}\right)\mathbb{P}\left(\delta_{k}^{s} = \beta\right)} \tag{B.4}$$

$$= \frac{\sum_{i=1}^{N_s}\sum_{j=1}^{N_s}\mathbb{P}\left(\delta_{k+1}^s = 1, \hat{\theta}_{k+1}^s = \hat{s}_\nu^s, \theta_{k+1}^s = s_j^s, \hat{\theta}_k^s = \hat{s}_\mu^s, \theta_k^s = s_i^s, \delta_k^s = \beta\right)}{\mathbb{P}\left(\hat{\theta}_k^s = \hat{s}_\mu^s\right)\mathbb{P}\left(\delta_k^s = \beta\right)}, \tag{B.5}$$

where commas indicate the intersections of events. (B.1) is due to (30). (B.2) relies on the definition of conditional probability. (B.3) uses the commutative property of the set intersection. From the definition of an FSMC in (1)–(5), as summarized in Fig. 1, it follows that for all $t \in \mathbb{Z}^{0+}$ and $\lambda \in \{s, a\}$, $\hat{\theta}_t^\lambda$ and δ_t^λ are independent of each other and each depends only on θ_t^λ. Furthermore, for all $t \in \mathbb{Z}^+$, θ_t^λ depends only on θ_{t-1}^λ. Thus, (B.4) relies on the independence of δ_k^s from $\hat{\theta}_k^s$. Finally, (B.5) follows from the law of total probability.

By the chain rule of probability, the numerator of (B.5) equals (B.6):

$$\begin{aligned}&\sum_{i=1}^{N_s}\sum_{j=1}^{N_s}\mathbb{P}\left(\delta_{k+1}^s = 1 \mid \hat{\theta}_{k+1}^s = \hat{s}_\nu^s, \theta_{k+1}^s = s_j^s, \hat{\theta}_k^s = \hat{s}_\mu^s, \theta_k^s = s_i^s, \delta_k^s = \beta\right)\mathbb{P}\left(\hat{\theta}_{k+1}^s = \hat{s}_\nu^s \mid \theta_{k+1}^s = s_j^s, \hat{\theta}_k^s = \hat{s}_\mu^s, \theta_k^s = s_i^s, \delta_k^s = \beta\right)\\ &\cdot \mathbb{P}\left(\theta_{k+1}^s = s_j^s \mid \hat{\theta}_k^s = \hat{s}_\mu^s, \theta_k^s = s_i^s, \delta_k^s = \beta\right)\mathbb{P}\left(\hat{\theta}_k^s = \hat{s}_\mu^s \mid \theta_k^s = s_i^s, \delta_k^s = \beta\right)\mathbb{P}\left(\theta_k^s = s_i^s \mid \delta_k^s = \beta\right)\mathbb{P}\left(\delta_k^s = \beta\right).\end{aligned} \tag{B.6}$$

From the definition of an FSMC presented above, δ_{k+1}^s in (B.6) depends only on θ_{k+1}^s. Likewise, $\hat{\theta}_{k+1}^s$ in the second factor in (B.6) depends only on θ_{k+1}^s, which in turn depends only on θ_k^s in the third factor in (B.6). $\hat{\theta}_k^s$ in the fourth factor in (B.6) depends only on θ_k^s, which is independent of δ_k^s in the fifth factor in (B.6). Consequently, (B.6) equals

$$\begin{aligned}&\sum_{i=1}^{N_s}\sum_{j=1}^{N_s}\mathbb{P}\left(\delta_{k+1}^s = 1 \mid \theta_{k+1}^s = s_j^s\right)\mathbb{P}\left(\hat{\theta}_{k+1}^s = \hat{s}_\nu^s \mid \theta_{k+1}^s = s_j^s\right)\mathbb{P}\left(\theta_{k+1}^s = s_j^s \mid \theta_k^s = s_i^s\right)\mathbb{P}\left(\hat{\theta}_k^s = \hat{s}_\mu^s \mid \theta_k^s = s_i^s\right)\mathbb{P}\left(\theta_k^s = s_i^s\right)\mathbb{P}\left(\delta_k^s = \beta\right)\\ &= \sum_{i=1}^{N_s}\sum_{j=1}^{N_s}\hat{\delta}_j^s\alpha_{j\nu}^s p_{ij}^s \alpha_{i\mu}^s \pi_i^s(k)\,\mathbb{P}\left(\delta_k^s = \beta\right) &\text{(B.7)}\\ &= \sum_{i=1}^{N_s}\sum_{j=1}^{N_s}\alpha_{i\mu}^s \pi_i^s(k) p_{ij}^s \hat{\delta}_j^s \alpha_{j\nu}^s\,\mathbb{P}\left(\delta_k^s = \beta\right) &\text{(B.8)}\\ &= \hat{e}_\mu^{s\top} P_e^{s\top} P_\pi^s(k) P_s^s P_e^s \hat{e}_\nu^s\,\mathbb{P}\left(\delta_k^s = \beta\right) &\text{(B.9)}\end{aligned}$$

(B.7) is obtained from (2), (5), (1), and (4). (B.8) relies on the commutative property of the scalar product. Finally, (B.9) follows from (5), (7), (3), and the definition of matrix multiplication.

By the law of total probability and the chain rule of probability, the denominator in (B.5) equals (B.10):

$$\begin{aligned}&\sum_{i=1}^{N_s}\mathbb{P}\left(\hat{\theta}_k^s = \hat{s}_\mu^s \mid \theta_k^s = s_i^s\right)\mathbb{P}\left(\theta_k^s = s_i^s\right)\mathbb{P}\left(\delta_k^s = \beta\right) &\text{(B.10)}\\ &= \sum_{i=1}^{N_s}\alpha_{i\mu}^s \pi_i^s(k)\,\mathbb{P}\left(\delta_k^s = \beta\right) &\text{(B.11)}\\ &= \hat{e}_\mu^{s\top} P_e^{s\top} P_\pi^s(k)\mathbf{1}\,\mathbb{P}\left(\delta_k^s = \beta\right). &\text{(B.12)}\end{aligned}$$

(B.11) is obtained from (4) and (5). (B.12) follows from (5), (7), and the definition of matrix multiplication.

Finally, by combining (B.9) with (B.12) and simplifying the resulting fraction by the common factor $\mathbb{P}\left(\delta_k^s = \beta\right)$, we obtain the first Eq. (31) in its final form.

The derivation of the second equation in (31) follows the same steps and is therefore omitted. □

Appendix C. Proof of Corollary 1

Under perfect CSI, $M_s = N_s$, $P_e^s = I_{N_s}$, implying that $\hat{e}_\mu^{s\top} P_e^{s\top} P_\pi^s(k) P_s^s P_e^s \hat{e}_\nu^s = \pi_i^s(k) p_{ij}^s \hat{\delta}_j^s$, $\hat{e}_\mu^{s\top} P_e^{s\top} P_\pi^s(k)\mathbf{1} = \pi_i^s(k)$, and $\hat{e}_\mu^{s\top} P_e^{s\top} P_\pi^s(k) P_f^s P_e^s \hat{e}_\nu^s = \pi_i^s(k) p_{ij}^s\left(1 - \hat{\delta}_j^s\right)$. The final expressions follow from simplifying the fractions by the common factor $\pi_i^s(k)$. □

Appendix D. Proof of Corollary 2

Without CSI, $M_s = 1$, $P_e^s = \mathbf{1}$, $\hat{e}_\mu^s = 1$, $\hat{e}_\nu^s = 1$, and $\mathbf{1}^\top P_\pi^s(k)\mathbf{1} = \sum_{i=1}^{N_s}\pi_i^s(k) = 1$. □

Appendix E. Proof of Proposition 3

It is similar to the proof of Proposition 2 in Appendix B. Consequently, we outline only the main steps. We focus on the first equation in (34). From (30), the law of total probability, and the chain rule of probability, we obtain (E.1):

$$\mathbb{P}\left(\eta_k^s = \left(1, \hat{s}_\mu^s\right)\right) = \sum_{i=1}^{N_s}\mathbb{P}\left(\delta_k^s = 1 \mid \hat{\theta}_k^s = \hat{s}_\mu^s, \theta_k^s = s_i^s\right)\mathbb{P}\left(\hat{\theta}_k^s = \hat{s}_\mu^s \mid \theta_k^s = s_i^s\right)\mathbb{P}\left(\theta_k^s = s_i^s\right) \tag{E.1}$$

$$= \sum_{i=1}^{N_s} \hat{\delta}_i^s \alpha_{i\mu}^s \pi_i^s(k). \tag{E.2}$$

From the definition of an FSMC, as in (1)–(5), δ_k^s depends only on θ_k^s and is therefore independent of $\hat{\theta}_k^s$. Consequently, (E.2) follows from (2), (5), and (4). The final form of the first equation in (34) is derived from (7) and the definition of matrix multiplication. The derivation of the second equation in (34) is similar and therefore omitted. □

Appendix F. Proof of Theorem 1

The intuition behind this proof is that the general MJLS theory in [12] applies to the system under consideration. The results in [12] show that, under technical assumptions compatible with our Assumptions 1–4 and the information set (16b)–(16c), the optimal SE has a structure similar to (23)–(26). The main difference is that the control inputs defined by (15) are not part of the filter's information set defined by (16b)–(16c). However, Proposition 1 addresses this difference. [12] shows that the SE's prediction and correction gains are related to the solution of filtering CRDEs and provides expressions for them. Consequently, the expressions for the prediction and correction gains of the SE for the system under consideration are also related to the solution of filtering CRDEs specialized to the problem at hand. The main technical challenge is to find an appropriate representation of the system (8)–(15), constrained by (1)–(6), and its SE within the MJLS framework, and to ensure that all necessary assumptions hold.

This proof comprises three stages. In the first stage, we show that the SE in (23)–(26) for the system (8)–(15), constrained by (1)–(6), and its simplified version without control input share the same error dynamics, as described by (28) and (29). The two versions of the SE differ only by a constant term that does not affect the SEs' error dynamics. Therefore, the optimal prediction and correction gains that minimize the mean-square error of the estimate in the simplified version also minimize it in the original version. Thus, the second and third stages of the proof focus on the simplified SE. In the second stage, we provide the MJLS representation of the system (8)–(11), constrained by (1)–(6) and Assumptions 1–4, that satisfies all the necessary assumptions for a well-defined solution in [12]. In the final third stage, we specialize the solution in [12] to the problem at hand.

First stage: Consider the system (8)–(11) without control input, subject to (1)–(6), Assumptions 1–4, and the information set (16b)–(16c). Specifically, (8) changes to

$$x_{k+1} = Ax_k + w_k, \tag{F.1}$$

and the SE with

$$\bar{x}_k = A\bar{x}_{k-1} - G_{(k-1,\hat{\theta}_{k-1}^s)}(\hat{y}_{k-1} - \delta_{k-1}^s C\bar{x}_{k-1}), \tag{F.2}$$

(25), and (26) exhibits the error dynamics described by (28) and (29), as evident from (F.1), (10), (11), (F.2), and (26). The SE (23)–(26) for the system (8)–(15), constrained by (1)–(6) and Assumptions 1–4, and its simplified version (F.2), (25), and (26) for the system (9) and (F.1)–(11), under the same constraints, differ only by the term $BF\check{u}_{k-1}$, which does not affect the error dynamics in (28) and (29). Therefore, both versions of the SE share the same optimal prediction and correction gains that minimize the mean-square error of the estimate. Consequently, we can focus on the simplified setting without a control input to derive expressions for the optimal prediction and correction gains.

Second stage: We show that the system (9) and (F.1)–(11), constrained by (1)–(6) and Assumptions 1–4, can be viewed as an MJLS, and that the SE (F.2), (25), and (26) can be viewed as its corresponding prediction–correction filter, which is optimal among Markovian filters. The operational modes of this MJLS are governed by the Markov chain $\{\eta_k^s\}$, with discrete states (30), transition probabilities (31), and state probabilities (34).

We recast the descriptions of the process noise $\{w_k\}$, the measurement noise $\{v_k\}$, and the related Assumptions 3 and 4 in the form used in [12,13] to facilitate adapting their results to the problem at hand. As white-noise sequences $\{w_k\}$ and $\{v_k\}$ have uncorrelated samples with zero mean, that is, $\forall t, \kappa \in \mathbb{Z}^{0+}$ such that $t \leq T$ and $\kappa \leq T$, it holds that $\mathbb{E}(w_t) = \mathbf{0}$, $\mathbb{E}(v_t) = \mathbf{0}$, $\mathbb{E}(w_t w_\kappa^\top) = 0$, and $\mathbb{E}(v_t v_\kappa^\top) = 0$ for $\kappa \neq t$, where 0 denotes zero matrices of the appropriate sizes. From the definition of the covariance matrix and the zero-mean property of the white-noise sequences, we have $\mathbb{E}(w_k w_k^\top) = \Sigma_w$ and $\mathbb{E}(v_k v_k^\top) = \Sigma_v$. For any set $\mathbb{S}$ in the event space $\mathcal{F}$ of a probability space $(\Omega, \mathcal{F}, \mathbb{P})$, we use the standard definition of the indicator function $1_{\mathbb{S}}$: for any sample υ in the sample space Ω,

$$1_{\mathbb{S}}(\upsilon) = \begin{cases} 1 & \text{if } \upsilon \in \mathbb{S} \\ 0 & \text{otherwise.} \end{cases} \tag{F.3}$$

Notably, $\mathbb{E}(1_{\mathbb{S}}(\upsilon)) = \mathbb{P}(\mathbb{S})$. By Assumption 3, $\{w_k\}$ and $\{v_k\}$ are independent of each other and of $\{\theta_k^s\}$, $\{\delta_k^s\}$, and $\{\hat{\theta}_k^s\}$. Therefore, from (30), $\{w_k\}$, $\{v_k\}$, and $\{\eta_k^s\}$ are independent, and

$$\mathbb{E}\left(w_k w_k^\top 1_{\left\{\eta_k^s = (\beta, \hat{s}_\mu^s)\right\}}\right) = \mathbb{E}(w_k w_k^\top)\,\mathbb{E}\left(1_{\left\{\eta_k^s = (\beta, \hat{s}_\mu^s)\right\}}\right) = \Sigma_w \mathbb{P}\left(\eta_k^s = (\beta, \hat{s}_\mu^s)\right) = \Sigma_w \omega_{(k,\beta,\mu)}^s, \tag{F.4}$$

$$\mathbb{E}\left(v_k v_k^\top 1_{\left\{\eta_k^s = (\beta, \hat{s}_\mu^s)\right\}}\right) = \mathbb{E}(v_k v_k^\top)\,\mathbb{E}\left(1_{\left\{\eta_k^s = (\beta, \hat{s}_\mu^s)\right\}}\right) = \Sigma_v \mathbb{P}\left(\eta_k^s = (\beta, \hat{s}_\mu^s)\right) = \Sigma_v \omega_{(k,\beta,\mu)}^s. \tag{F.5}$$

The last equality in (F.4) and the last equality in (F.5) follow from Proposition 3 and (35). By the same argument,

$$\mathbb{E}\left(w_k 1_{\left\{\eta_k^s=(\beta,\hat{s}_\mu^s)\right\}}\right)=\mathbf{0},\quad \mathbb{E}\left(v_k 1_{\left\{\eta_k^s=(\beta,\hat{s}_\mu^s)\right\}}\right)=\mathbf{0},\quad \mathbb{E}\left(w_k v_k^\top 1_{\left\{\eta_k^s=(\beta,\hat{s}_\mu^s)\right\}}\right)=0,\quad \mathbb{E}\left(v_k w_k^\top 1_{\left\{\eta_k^s=(\beta,\hat{s}_\mu^s)\right\}}\right)=0. \tag{F.6}$$

In line with [12, Assumptions (A1)–(A3)], we can obtain the same results starting from a single wide-sense white noise sequence in $\mathbb{R}^{n_w}$, denoted by $\{\tilde{w}_k\}$.

[12, Assumption (A1)] states that $\forall t,\kappa\in\mathbb{Z}^{0+}$ such that $t\le T$ and $\kappa\le T$, it holds that $\mathbb{E}(\tilde{w}_t)=\mathbf{0}$, $\mathbb{E}(\tilde{w}_t\tilde{w}_t^\top)=I_{n_w}$, and $\mathbb{E}(\tilde{w}_t\tilde{w}_\kappa^\top)=0$ for $\kappa\neq t$. Thus, instead of $\{w_k\}$ and $\{v_k\}$ above, we can consider $\{\tilde{w}_k\}$ that satisfies [12, Assumption (A1)] along with some additional properties below.

Assumption 3 yields [12, Assumption (A3)], which states that the noise $\{\tilde{w}_k\}$ and the initial condition x_0 are independent of the Markov chain $\{\eta_k^s\}$. In addition, it states that $\{\tilde{w}_k\}$ and x_0 are uncorrelated, i.e., $\mathbb{E}(\tilde{w}_k x_0^\top)=0$. Assumption 3 regarding the noise process (applied to $\{\tilde{w}_k\}$ rather than $\{w_k\}$ and $\{v_k\}$) states that it is independent of $\{\theta_k^s\}$, $\{\delta_k^s\}$, and $\{\hat{\theta}_k^s\}$, thereby implying independence of $\{\eta_k^s\}$. Furthermore, it states that the noise ($\{\tilde{w}_k\}$) is independent of x_0, implying that $\{\tilde{w}_k\}$ and x_0 are uncorrelated. Finally, it also states that x_0 is independent of $\{\theta_k^s\}$, $\{\hat{\theta}_k^s\}$ and $\{\delta_k^s\}$, and hence of $\{\eta_k^s\}$.

The last remaining [12, Assumption (A2)] concerns operational-mode-dependent covariances, the independence of process and measurement noises, and the invertibility of certain matrices. To state this assumption formally, we first need to complete the description of the MJLS. As a covariance matrix, $\Sigma_w\succeq 0$ and can always be decomposed as $\Sigma_w=\Gamma_w\Gamma_w^\top$, for instance, via the Cholesky factorization. Similarly, Σ_v can also always be decomposed as $\Sigma_v=\Gamma_v\Gamma_v^\top$. Assuming $\Gamma_w\Gamma_v^\top=0$ — which corresponds to the $\{w_k\}$ independence of $\{v_k\}$, as per Assumption 3 — alongside [12, Assumptions (A1) and (A3)], we can use $\Gamma_w\tilde{w}_k$ instead of w_k and $\Gamma_v\tilde{w}_k$ instead of v_k to derive (F.4)–(F.6):

$$\mathbb{E}\left(\Gamma_w\tilde{w}_k\left(\Gamma_w\tilde{w}_k\right)^\top 1_{\left\{\eta_k^s=(\beta,\hat{s}_\mu^s)\right\}}\right)=\mathbb{E}\left(\Gamma_w\tilde{w}_k\tilde{w}_k^\top\Gamma_w^\top\right)\mathbb{E}\left(1_{\left\{\eta_k^s=(\beta,\hat{s}_\mu^s)\right\}}\right)=\Gamma_w\mathbb{E}\left(\tilde{w}_k\tilde{w}_k^\top\right)\Gamma_w^\top\omega_{(k,\beta,\mu)}^s=\Gamma_w I_{n_w}\Gamma_w^\top\omega_{(k,\beta,\mu)}^s=\Sigma_w\omega_{(k,\beta,\mu)}^s,$$

$$\mathbb{E}\left(\Gamma_v\tilde{w}_k\left(\Gamma_v\tilde{w}_k\right)^\top 1_{\left\{\eta_k^s=(\beta,\hat{s}_\mu^s)\right\}}\right)=\Gamma_v\mathbb{E}\left(\tilde{w}_k\tilde{w}_k^\top\right)\Gamma_v^\top\mathbb{P}\left(\eta_k^s=(\beta,\hat{s}_\mu^s)\right)=\Gamma_v\Gamma_v^\top\omega_{(k,\beta,\mu)}^s=\Sigma_v\omega_{(k,\beta,\mu)}^s,$$

$$\mathbb{E}\left(\Gamma_w\tilde{w}_k 1_{\left\{\eta_k^s=(\beta,\hat{s}_\mu^s)\right\}}\right)=\mathbf{0},\quad \mathbb{E}\left(\Gamma_v\tilde{w}_k 1_{\left\{\eta_k^s=(\beta,\hat{s}_\mu^s)\right\}}\right)=\mathbf{0},\quad \mathbb{E}\left(\Gamma_w\tilde{w}_k\left(\Gamma_v\tilde{w}_k\right)^\top 1_{\left\{\eta_k^s=(\beta,\hat{s}_\mu^s)\right\}}\right)=0,\quad \mathbb{E}\left(\Gamma_v\tilde{w}_k\left(\Gamma_w\tilde{w}_k\right)^\top 1_{\left\{\eta_k^s=(\beta,\hat{s}_\mu^s)\right\}}\right)=0.$$

For all $\beta\in\{0,1\}$ and $\hat{s}_\mu^s\in\hat{\mathcal{S}}_s$, we set $\mathbf{A}_{(\beta,\hat{s}_\mu^s)}=A$, $\mathbf{B}_{(\beta,\hat{s}_\mu^s)}=\Gamma_w$, $\mathbf{C}_{(\beta,\hat{s}_\mu^s)}=\beta C$, and $\mathbf{D}_{(\beta,\hat{s}_\mu^s)}=\beta\Gamma_v$, yielding the following MJLS.

$$\begin{cases} x_{k+1}=\mathbf{A}_{\eta_k}x_k+\mathbf{B}_{\eta_k}\tilde{w}_k,\\ \hat{y}_k=\mathbf{C}_{\eta_k}x_k+\mathbf{D}_{\eta_k}\tilde{w}_k,\\ \mathbb{E}(x_0)=\mathrm{x}_0,\ \mathbb{E}(x_0x_0^\top)=\mathrm{X}_0. \end{cases} \tag{F.7}$$

By construction, (F.7), together with (30), (31), and (34) describes the dynamics of the system defined by (9) and (F.1)–(11), subject to (1)–(6). As noted before, we use $\mathbf{B}_{\eta_k}\tilde{w}_k$ instead of w_k and $\mathbf{D}_{\eta_k}\tilde{w}_k$ instead of $\delta_k^s v_k$ solely to demonstrate the full compatibility of the results in [12] with the problem at hand. The same solution can be obtained by setting $x_{k+1}=\mathbf{A}_{\eta_k}x_k+w_k$ and $\hat{y}_k=\mathbf{C}_{\eta_k}x_k+\tilde{\mathbf{D}}_{\eta_k}v_k$, with $\tilde{\mathbf{D}}_{(\beta,\hat{s}_\mu^s)}=\beta$ for all $\beta\in\{0,1\}$ and $\hat{s}_\mu^s\in\hat{\mathcal{S}}_s$. By [12, Theorem 4], the optimal Markovian filter for the MJLS (F.7) is the following prediction–correction filter.

$$\begin{cases} \bar{x}_{k+1}=\mathbf{A}_{\eta_k}\bar{x}_k-\bar{\mathbf{M}}_{(k,\eta_k)}\left(\hat{y}_k-\mathbf{C}_{\eta_k}\bar{x}_k\right),\\ \hat{x}_k=\bar{x}_k-\hat{\mathbf{M}}_{(k,\eta_k)}\left(\hat{y}_k-\mathbf{C}_{\eta_k}\bar{x}_k\right),\\ \bar{x}_0=\mathbb{E}(x_0)=\mathrm{x}_0. \end{cases} \tag{F.8}$$

We note that (F.7) and (F.8), with $\mathbf{C}_{(\beta,\hat{s}_\mu^s)}=\beta C$ and $\mathbf{D}_{(\beta,\hat{s}_\mu^s)}=\beta\Gamma_v$, express a fundamental *structural property*: if $\beta=0$, then $\eta_k=(0,\hat{s}_\mu^s)$ implies $\mathbf{C}_{(0,\hat{s}_\mu^s)}=0$ and $\mathbf{D}_{(0,\hat{s}_\mu^s)}=0$, so $\hat{y}_k=\mathbf{0}$ and $\left(\hat{y}_k-\mathbf{C}_{(0,\hat{s}_\mu^s)}\bar{x}_k\right)=\mathbf{0}$, and therefore $\bar{x}_{k+1}=A\bar{x}_k$ and $\hat{x}_k=\bar{x}_k$. Thus, the prediction and correction gains $\bar{\mathbf{M}}_{(k,0,\hat{s}_\mu^s)}$ and $\hat{\mathbf{M}}_{(k,0,\hat{s}_\mu^s)}$ are never applied and do not influence the SE error dynamics. Consequently, [12, Assumption (A2)] is relevant only to the operational modes with $\beta=1$. For an arbitrary MJLS, this assumption states that $\mathbf{B}_{(\beta,\hat{s}_\mu^s)}\mathbf{D}_{(\beta,\hat{s}_\mu^s)}^\top=0$ and $\mathbf{D}_{(\beta,\hat{s}_\mu^s)}\mathbf{D}_{(\beta,\hat{s}_\mu^s)}^\top\succ 0$ for each operational mode. The first part of [12, Assumption (A2)] concerns the independence of process and measurement noises, while the second ensures the invertibility of certain matrices required to solve the optimal filtering problem. These two properties are not required for $\beta=0$ because, in this case, the measurement noise does not contribute to $\hat{y}_k$, and there is no matrix inversion. For all $k\in\mathbb{Z}^{0+}$, $\bar{\mathbf{M}}_{(k,0,\hat{s}_\mu^s)}$ and $\hat{\mathbf{M}}_{(k,0,\hat{s}_\mu^s)}$ are not a part of the optimal filtering problem because they do not affect the SE error dynamics. As indicated above, Assumption 3 on the independence of measurement noise from process noise implies $\Gamma_w\Gamma_v^\top=0$, which is exactly the first part of [12, Assumption (A2)] for $\beta=1$: $\mathbf{B}_{(1,\hat{s}_\mu^s)}\mathbf{D}_{(1,\hat{s}_\mu^s)}^\top=\Gamma_w\Gamma_v^\top=0$. Furthermore, Assumption 4 corresponds to the second part of [12, Assumption (A2)], as $\mathbf{D}_{(\beta,\hat{s}_\mu^s)}\mathbf{D}_{(\beta,\hat{s}_\mu^s)}^\top=\Gamma_v\Gamma_v^\top=\Sigma_v\succ 0$.

Therefore, all assumptions in [12] are met. From (30) and the matrix assignments leading to (F.7), we have $\mathbf{A}_{\eta_k^s}=A$ and $\mathbf{C}_{\eta_k^s}=\delta_k^s C$. With $G_{(k,\hat{s}_\mu^s)}=\bar{\mathbf{M}}_{(k,1,\hat{s}_\mu^s)}$ and $\hat{G}_{(k,\hat{s}_\mu^s)}=\hat{\mathbf{M}}_{(k,1,\hat{s}_\mu^s)}$, (F.8) becomes a combination of (F.2), (25), and (26), with (F.2) rewritten for $\bar{x}_{k+1}$ and $\bar{x}_k$ instead of $\bar{x}_k$ and $\bar{x}_{k-1}$.

Third stage: The expressions for the prediction and correction gains in [12] are derived from the solutions to the filtering CRDEs, which describe the dynamics of the expected squared prediction error in each operational mode. For all $\beta \in \{0,1\}$ and $\hat{s}^s_\mu \in \hat{\mathcal{S}}_s$, $\bar{Y}_{(k,\beta,\mu)} = \mathbb{E}\left(\tilde{x}_k \tilde{x}_k^\top 1_{\left\{\eta_k^s=(\beta,\hat{s}^s_\mu)\right\}}\right)$, with $\tilde{x}_k$ defined by (27). For a generic MJLS without the structural property above, for all $\beta,\gamma \in \{0,1\}$ and $\hat{s}^s_\mu, \hat{s}^s_\nu \in \hat{\mathcal{S}}_s$,

$$\bar{Y}_{(k+1,\gamma,\nu)} = \sum_{\beta=0}^{1}\sum_{\mu=1}^{M_s} \varsigma^s_{(k,\mu,\gamma,\nu)}\left(\mathbf{A}_{(\beta,\hat{s}^s_\mu)}\bar{Y}_{(k,\beta,\mu)}\mathbf{A}^\top_{(\beta,\hat{s}^s_\mu)} - \mathbf{A}_{(\beta,\hat{s}^s_\mu)}\bar{Y}_{(k,\beta,\mu)}\mathbf{C}^\top_{(\beta,\hat{s}^s_\mu)}\mathbf{W}^{-1}_{(\beta,\hat{s}^s_\mu)}\mathbf{C}_{(\beta,\hat{s}^s_\mu)}\bar{Y}_{(k,\beta,\mu)}\mathbf{A}^\top_{(\beta,\hat{s}^s_\mu)} + \omega^s_{(k,\beta,\mu)}\mathbf{B}_{(\beta,\hat{s}^s_\mu)}\mathbf{B}^\top_{(\beta,\hat{s}^s_\mu)}\right),$$

$$\mathbf{W}_{(\beta,\hat{s}^s_\mu)} = \omega^s_{(k,\beta,\mu)}\mathbf{D}_{(\beta,\hat{s}^s_\mu)}\mathbf{D}^\top_{(\beta,\hat{s}^s_\mu)} + \mathbf{C}_{(\beta,\hat{s}^s_\mu)}\bar{Y}_{(k,\beta,\mu)}\mathbf{C}^\top_{(\beta,\hat{s}^s_\mu)},$$

$$\bar{Y}_{(0,\beta,\mu)} = \omega^s_{(0,\beta,\mu)}\left(\mathrm{X}_0 - \mathrm{x}_0\mathrm{x}_0^\top\right).$$

Furthermore, the prediction and correction gains are as follows.

$$\hat{\mathbf{M}}_{(k,\beta,\hat{s}^s_\mu)} = -\bar{Y}_{(k,\beta,\mu)}\mathbf{C}^\top_{(\beta,\hat{s}^s_\mu)}\mathbf{W}^{-1}_{(\beta,\hat{s}^s_\mu)}, \quad \bar{\mathbf{M}}_{(k,\beta,\hat{s}^s_\mu)} = \mathbf{A}_{(\beta,\hat{s}^s_\mu)}\hat{\mathbf{M}}_{(k,\beta,\hat{s}^s_\mu)}.$$

Accounting for $\beta = 0$ and the matrix assignments used to obtain the MJLS representation, (37)–(39) follow. Likewise, the expression for the optimal cost (40) follows from [12, Theorem 4], its proof, and the structural property above. □

Appendix G. Proof of Theorem 2

From the first two stages of the proof of Theorem 1, the system (8)–(15), under Assumptions 1–5, the information set (16b)–(16c), and the communication links from (1)–(6), with the time-invariant SE described by (23)–(25), is an MJLS. Therefore, we can apply the infinite-horizon filtering results of [12] to derive the CAREs expressed by (37)–(39b) with ∞ instead of k. Intuitively, it relies on standard results from the general MJLS theory regarding the convergence of the CRDEs to CAREs, which requires MS detectability from Definition 2 [13, Sections A.1–A.4]. The derivation of LMIs follows the standard procedure used in the proof of [13, Theorem A.12]. □

Appendix H. Proof of Proposition 4

We can repeat the steps in the proof of Theorem 1 to show that the closed-loop system is an MJLS. Then, the general procedure in [13, Sections 3.2 and 3.5] applies, and the result follows from the assignments used to construct the MJLS representation. □

Data availability

Data will be made available on request.

References

[1] P. Park, S.C. Ergen, C. Fischione, C. Lu, K.H. Johansson, Wireless network design for control systems: A survey, IEEE Commun. Surv. Tut. 20 (2) (2018) 978–1013.

[2] W. Liu, G. Nair, Y. Li, D. Nesic, B. Vucetic, H.V. Poor, On the latency, rate, and reliability tradeoff in wireless networked control systems for IIoT, IEEE Internet Things J. 8 (2) (2021) 723–733.

[3] M. Pezzutto, S. Dey, E. Garone, K. Gatsis, K.H. Johansson, L. Schenato, Wireless control: Retrospective and open vistas, Annu. Rev. Control. 58 (2024) 100972.

[4] Y. Zacchia Lun, F. Smarra, A. D'Innocenzo, Optimal control over Markovian wireless communication channels under generalized packet dropout compensation, Automatica 176 (2025) 112240.

[5] Y. Zacchia Lun, F. Santucci, A. D'Innocenzo, Wireless control with channel state detection and message dropout compensation, IEEE Control. Syst. Lett. 9 (2025) 1399–1404.

[6] O.L.d.V. Costa, M.D. Fragoso, M.G. Todorov, A detector-based approach for the H_2 control of Markov jump linear systems with partial information, IEEE Trans. Autom. Control 60 (5) (2015) 1219–1234.

[7] A.M. de Oliveira, O.L.d.V. Costa, Mixed $\mathcal{H}_2/\mathcal{H}_\infty$ control of hidden Markov jump systems, Int. J. Robust Nonlin. Control. 28 (4) (2018) 1261–1280.

[8] A. Impicciatore, Y. Zacchia Lun, P. Pepe, A. D'Innocenzo, Optimal output-feedback control over Markov wireless communication channels, IEEE Trans. Autom. Control 69 (3) (2024) 1643–1658.

[9] P. Sadeghi, R. Kennedy, P. Rapajic, R. Shams, Finite-state Markov modeling of fading channels–A survey of principles and applications, IEEE Signal Process. Mag. 25 (5) (2008) 57–80.

[10] Y. Zacchia Lun, C. Rinaldi, A. D'Innocenzo, F. Santucci, Co-designing wireless networked control systems on IEEE 802.15.4-based links under Wi-Fi interference, IEEE Access 12 (2024) 71157–71183.

[11] M.A. Khan, Y. Zacchia Lun, P. Di Marco, A. Mahmood, F. Santucci, M. Gidlund, Analysis of communication and control performance of multi-hop IEEE 802.15.4-based WNCSs under Wi-Fi interference, in: IEEE Int. Conf. Factory Commun. Syst., WFCS, IEEE, 2025, pp. 1–8.

[12] O.L.d.V. Costa, A.M. de Oliveira, Prediction–correction filtering for discrete-time Markov jump linear systems, J. Control. Autom. Electr. Syst. 35 (2) (2024) 291–300.

[13] O.L.d.V. Costa, M.D. Fragoso, R.P. Marques, Discrete-Time Markov Jump Linear Systems, Springer, 2005.

[14] A.N. Vargas, L. Acho, G. Pujol, E.F. Costa, J.Y. Hishihara, J.B.R. do Val, Output feedback of Markov jump linear systems with no mode observation: An automotive throttle application, Internat. J. Robust Nonlinear Control 26 (2016) 1980–1993.

[15] Y. Zacchia Lun, F. Santucci, A. D'Innocenzo, Robust linear quadratic regulation over polytopic time-inhomogeneous Markovian channels under generalized packet dropout compensation, IEEE Control. Syst. Lett. 8 (2024) 3315–3320.